

Time Series Analysis of terrain and climatic parameters data retrieved from Terraclimate dataset: A case study in Ranchi and Khunti district, Jharkhand, India

Yajnavalkya Bandyopadhyay¹, Nilanchal Patel²

¹ M.Tech Student, Department of Remote Sensing, Birla Institute of Technology, Mesra, Ranchi, Jharkhand, India

ORCID - <https://orcid.org/0000-0001-8379-5491>

email – yajnab@gmail.com

² Professor, Department of Remote Sensing, Birla Institute of Technology, Mesra, Ranchi, Jharkhand, India

Peer-Reviewed status

This article is a non-peer reviewed preprint submitted to EarthArXiv and will be peer reviewed by Springer Nature.

Abstract

Climatic and Terrain parameters which include the soil moisture, precipitation, evapotranspiration, maximum and minimum temperature are the most crucial factors which drives the future of earth. Soil Moisture regulates the movement of water and heat energy between the land surface and the atmosphere through evaporationn and plant transpiration. Precipitation controls the entire operation of the hydrosphere. Evapotranspiration is crucial for agricultural irrigation and water resource management. Land surface temperature (LST), which is crucial for monitoring crop and vegetation health, calculating the net radiation budget at the Earth's surface. The parameters of the delineated study area (Ranchi and Khunti districts, Jharkhand, India) data were retrieved

from Terraclimate dataset for the years 1990 - 2020. The dataset was refined, and Mann Kendall trend analysis was implemented, and the trend graphs were prepared to determine the change in trend and relationship. The graphs generated shows the changes (positive or negative) in trend in every pixel for the 31 years for every month.

Keywords : Climate Factor, Terrain Parameter, Trend Analytics, Mann-Kendall Test

1.1 Introduction

Several research have looked into the critical problem of rainfall trends in India over the last century. Seasonal and inter-annual fluctuation in real evapotranspiration (ET) has a big impact on vegetation dynamics and land surface hydrology. As per the studies, the fluctuation in time of condition of climate shows significant results on evapotranspiration. Evapotranspiration dynamics and interaction of it with its variables referring to climate shows critical finding for future forecasting. Many regional studies performed so far have demonstrated the importance of evapotranspiration and its climate change effect.

Soil moisture is an important parameter for hydrological research (S. Unninayar, L.M. Olsen, 2015). At low relative humidity the soil moisture content depends on the absorbed moisture content. At higher relative humidity it depends on the pore size. Plants require the soil moisture for their growth and when the content is low it is in the form of the thin film. It dissolves the salt and makes the soil solution which is required for the plant growth. Aggregation qualities and colloidal properties makes the soil to hold water by holding water on the surface of the pores, colloids and other particles. The forces responsible to do this are surface tension and surface attraction and are known as soil moisture tension which is referred to concept of energy in moisture retention relationships. The force with which water is held is also termed as suction. Time series

analysis of the hydrological parameter and soil moisture will enable us to know how the trend in the soil moisture changed in different time scales viz. months and years in relation to the other hydrological parameters. Mann-Kendall analysis has also been performed to determine the trend.

Agriculture in Jharkhand is primarily rain fed, and is grown on undulating topography associated with shallow soil depth, low water retentive capacity, poor soil fertility, and fragmented holdings with little irrigation possibilities (10-12 percent). The appropriateness, adaptability, and production of crops in a specific region are influenced by rainfall and temperature. According to the Intergovernmental Panel on Climate Change, billions of people, particularly in developing countries, will suffer modifications in rainfall styles, to be able to make a contribution to intense water shortages or flooding, in addition to growing temperatures, to be able to manage cropping styles and developing seasons to shift.

University of California, Merced has developed a dataset called Terraclimate having data from the year of 1958-2021 with a monthly temporal resolution and a spatial resolution of ~4km. The parameters of soil moisture, precipitation, evapotranspiration and temperature are retrieved from there.

The intensity and frequency of extremes may be effortlessly modified with the aid of using weather alternate and the modifications in weather extremes and their affects on quite a few bodily and organic structures tested with the aid of using the Intergovernmental Panel on Climate Change (IPCC) and their results also can make a contribution to worldwide warming (IPCC 2007). Many elements consisting of the enlargement of cities, and rapid populace increase induce alongside migration from rural to city regions pose a chief task for town planners and additionally contributes to growing weather alternate. Some environmental hazards consisting of excessive temperature and severe rainfall, which leads to flooding in Addis Ababa, can be indicators of weather alternate (Birhanu et al. 2016). Also, the town temperature is often stricken by anthropogenic sports alongside weather alternate.

The objective of the present research is primarily two-fold. First objective comprises determination of the trend of the climatic and terrain parameters in the districts of Ranchi and Khunti by implementing Mann Kendall test, and the second objective investigates the interactive changes between the different parameters. The results derived from these investigations will aid the climatologists and planners to develop feasible strategies to alleviate the climate induced hazards in the study area.

1.2 Research Objectives:

As discussed earlier, the present study deals with the spatio-temporal variability analysis of two climatic parameters viz. precipitation, evapotranspiration and three terrain parameters viz. soil moisture, minimum and maximum land surface temperatures (LSTmin and LSTmax) over a period of 31 years from 1990 to 2020. The specific objectives of the present investigation include:

- 1.** To determine the month wise variation of the five individual parameters over a period of 372 months from the year 1990 to 2020 (31 years x 12 months = 372 months).
- 2.** To determine the monthly variation of the individual parameters in the respective calendar years starting from 1990 to 2020.
- 3. (a)** To determine the inter-quartile variability of the individual parameters over the entire year i.e., comprising 12 calendar months in the respective years, i.e. from 1990 to 2020.

(b) To determine the inter-quartile variability of the individual parameters over the entire period of study i.e., 1990 to 2020 (31 years) in the respective calendar months, i.e. January to December.

4. To determine the trend of the individual parameters in each pixel of the study area in the respective calendar months, i.e., from January to December, employing the Mann-Kendall trend analysis technique.

2.1 State of Art

JD Salas et. Al (1980.) showed that how the trend changes in the hydrological parameters which are precipitation and temperature variance. In the year of 1997 SG Giakoumakis et.al. showed the hydrological time series of Evinos river basin. In 2002 S Yue et.al. showed the rainfall and temperature time series and their autocorrelation. In 2003 Veli Hyvärinen et. al. explored the time variation of precipitation and evapotranspiration in Finland. Again in 2004 S Yue et. al. evaluated the Mann-Kendall test on serially correlated hydrological time series. M Kallache et. al. in 2005 checked trend assessment in Hydrology and Climate Research. Q Shao et. Al. in 2010 Showed trend detection in hydrological time series by segment regression with application to Shiyang River Basin. Time series analysis of the long-term hydrologic impacts of afforestation in the Águeda watershed of north-central Portugal was experimented in 2015 by D Hawtree.et al. In the year of 2022, Y Shea et.al. Showed Hydrological Time-series changes using Piecewise linear representation.

2.2 Study Area

The area selected for the present study comprises the Ranchi and Khunti districts of Jharkhand state of India.

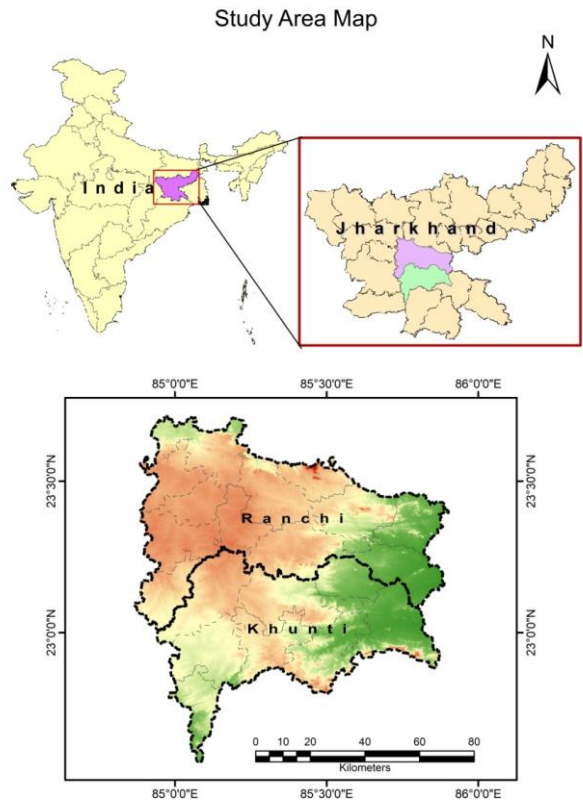


Figure 1: Study Area

The area comprises 337 pixels of 4 km resolution each. The residual type of soil is mostly found in the Ranchi and Khuti region. Archean and metamorphic rocks are highly exposed, and lateritic soils occur as a result of strong rainfall and high temperatures. The soils in the region are classed as follows based on texture: Stony and gravel soils, and are red or yellow. Soil is formed through the disintegration of crystalline metamorphic rocks like schist, slate, and gneiss. Alluvial soils are found in the region's river channels and consist primarily of coarse sand and gravels, as well as sediment and muck.

The study area falls under the Chotanagpur patland that resembles a table with steep edges all around and a flat top. The elevation ranges from 500 to 700 metres above sea level. Pat refers to a feature. The different landscape features in the study area are Scarps, revitalised meandering, Tors, are also prevalent in the state's beautiful landscape.

Virtually two-thirds of the study area is covered by nearly flat and very gently sloping land. The district's core section has a moderately sloping terrain. Strongly sloping to very steeply sloping ground may be found largely along the district's northern and southern limits, as well as in the eastern half.

The climate for the Ranchi and Khuti districts are classified as semi-arid subtropical. The average yearly temperature is 24.50°C, with a maximum of 280°C in the summer. Winter temperatures average 190 degrees Celsius. The area is classified as "hyperthermic" because the difference in mean summer and mean winter temperatures is greater than 50 degrees Celsius. The district receives about 1057.12 mm of rainfall every year, with the highest amounts falling in July and August and the lowest in November. However, rainfall is inconsistent, and droughts occur on a regular basis, roughly every other year.

In this districts, three types of forests: reserved, protected, and open forests covering an area of 7678 square kilometres. Dry Deciduous Forest comprise of Bamboobs, Amaltas, Semal, Plas, Khour, Mahua, Asan, Sabai and Khus grasses and others grow in this type of forest. b) Dry Peninsular Forest has sal, jack trees, bamboo thickets, and other trees and Moist Peninsular Forest: These types of forests are found at higher elevations where rainfall exceeds 2000 mm. In such woodlands, sal is the most prevalent tree. Shrubs and shrubs can be found in patches in hilly/rocky environments and stony wastelands. Accasia catechu (Khair), Zizyphys jujuba (Ber), Accasia arabica (Babul), neem (Azadirachta Indica), Shisam (Dalbergia Latifolia), Shuras (Albizzia Lebbeck) and other species are dominant throughout the region.

The primary river Subarnarekha flows through the region. Tributatiea such as Tazna, Kanchi, and Banai Rivers, Chhata, Karo, Changjhor, and Koel Rivers, are key tributary rivers that drain the basins in the region. Alluvial soils made up primarily of coarse sand and gravel mixed with silt and clay cover river channels throughout the district.

Agriculture and forests dominate the district's land use/cover. Other land use groups found in the district include wasteland, non-agricultural lands, pasture, cultivable wasteland, and fallow land.

2.3 Materials and Methods

Google Earth Engine was used for retrieving the terrain and climatic data for 31 years with temporal resolution of one month from Terraclimate that include Soil Moisture, Precipitation, Evapotranspiration, Highest and Lowest Soil Temperature. The data was refined and prepared for the analysis. The seasonality of the parameters was determined and Mann Kendall's Test was performed to determine the trend of the different parameters for the respective pixels over a period of 31 years.

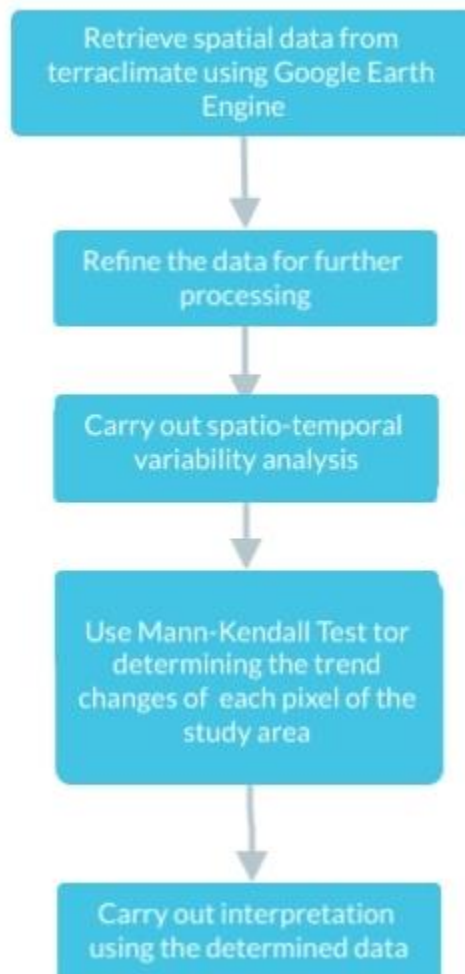


Figure 2: Methodology

Mann-Kendall's Test

Mann-Kendall test was formulated by Mann in 1945 for analyzing the trend mostly in environmental, climatological and hydrological data. The advantages of this test are its ability to handle data which are nonparametric and inhomogeneous in nature, that is, data which are not normally distributed and which are characterized by abrupt breaks. The H0 or null hypothesis represents no trend whereas the alternate hypothesis claims the data to have a trend. The calculation for Mann-Kendall test is as follows:

$$S = \sum_{k=1}^{n-1} \sum_{j=k+1}^n \text{sgn}(x_j - x_k)$$

The trend test is applied to a time series X_k , which is ranked from $k = 1, 2, 3, \dots, n-1$, which is ranked from $j = i + 1, i + 2, i + 3, \dots, n$. Each of the data points x_j is taken as a reference point.

$$\text{Sgn}(x_j - x_i) = \begin{cases} -1, & (x_j - x_i) < 0 \\ 0, & (x_j - x_i) = 0 \\ +1, & (x_j - x_i) > 0 \end{cases}$$

A positive S value indicates an upward trend, while a negative value indicates a downward trend. The variance of S for the trend is calculated as follows :

$$\text{Var}(S) = \frac{n(n-1)(2n+5) + \sum_{i=1}^m t_i(t_i-1)(2t_i+5)}{18}$$

3.1 Results

3.1.1 Soil Moisture

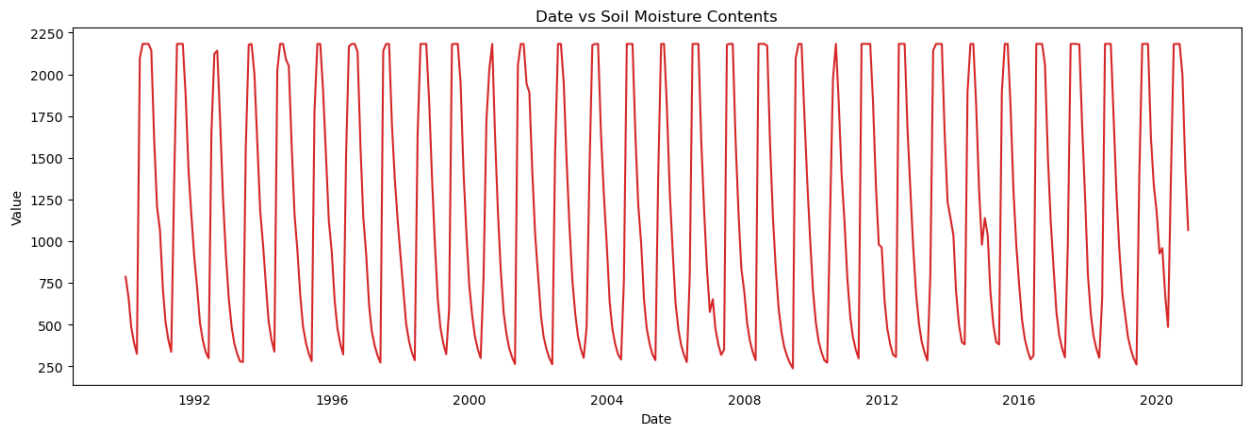


Figure 3: Soil Moisture Trend

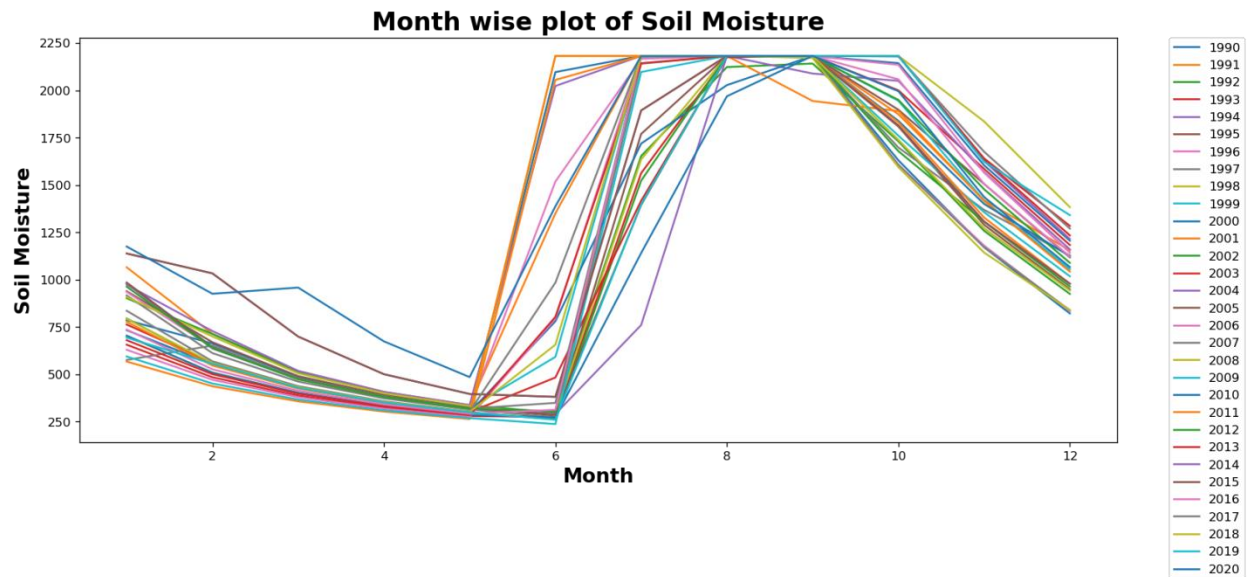


Figure 4: Month Wise plot of Soil Moisture

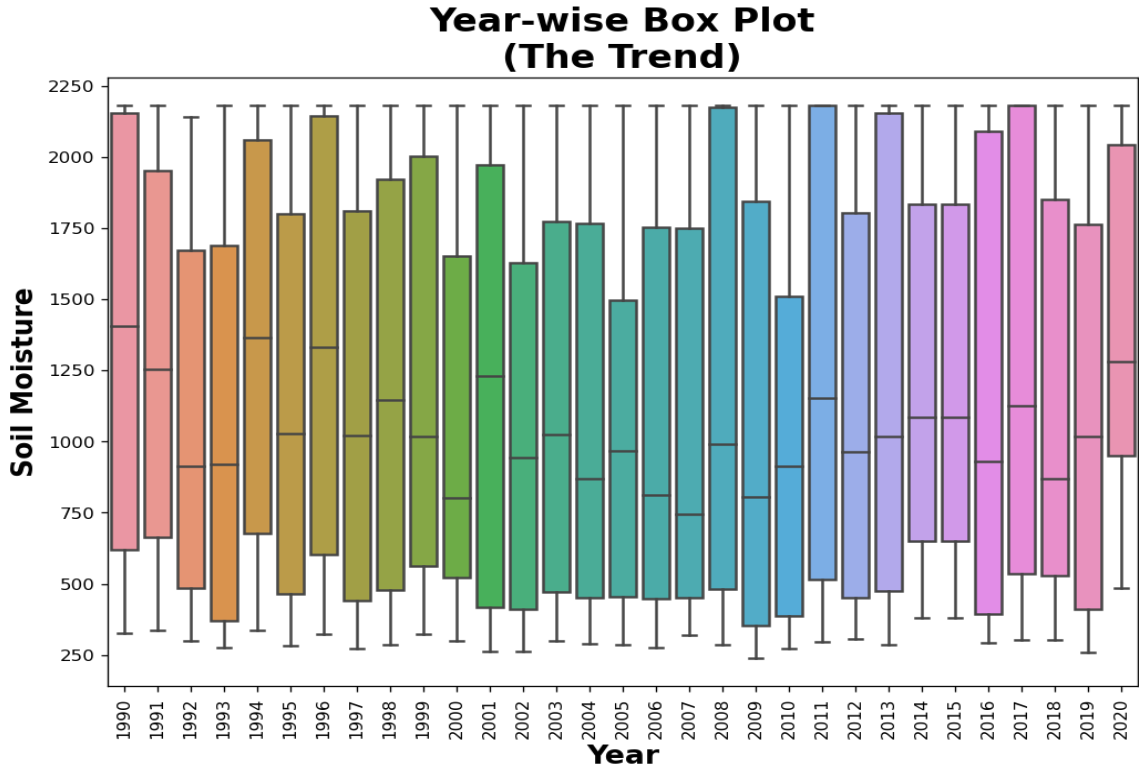


Figure 5: Year Wise Box Plot of Soil Moisture

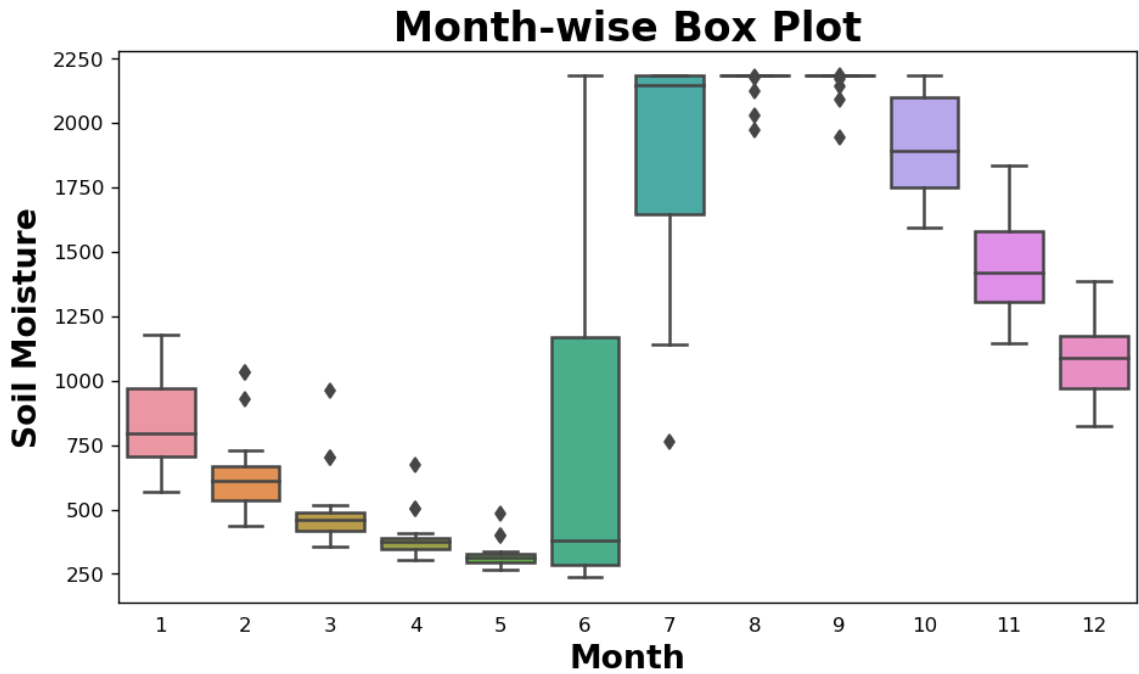


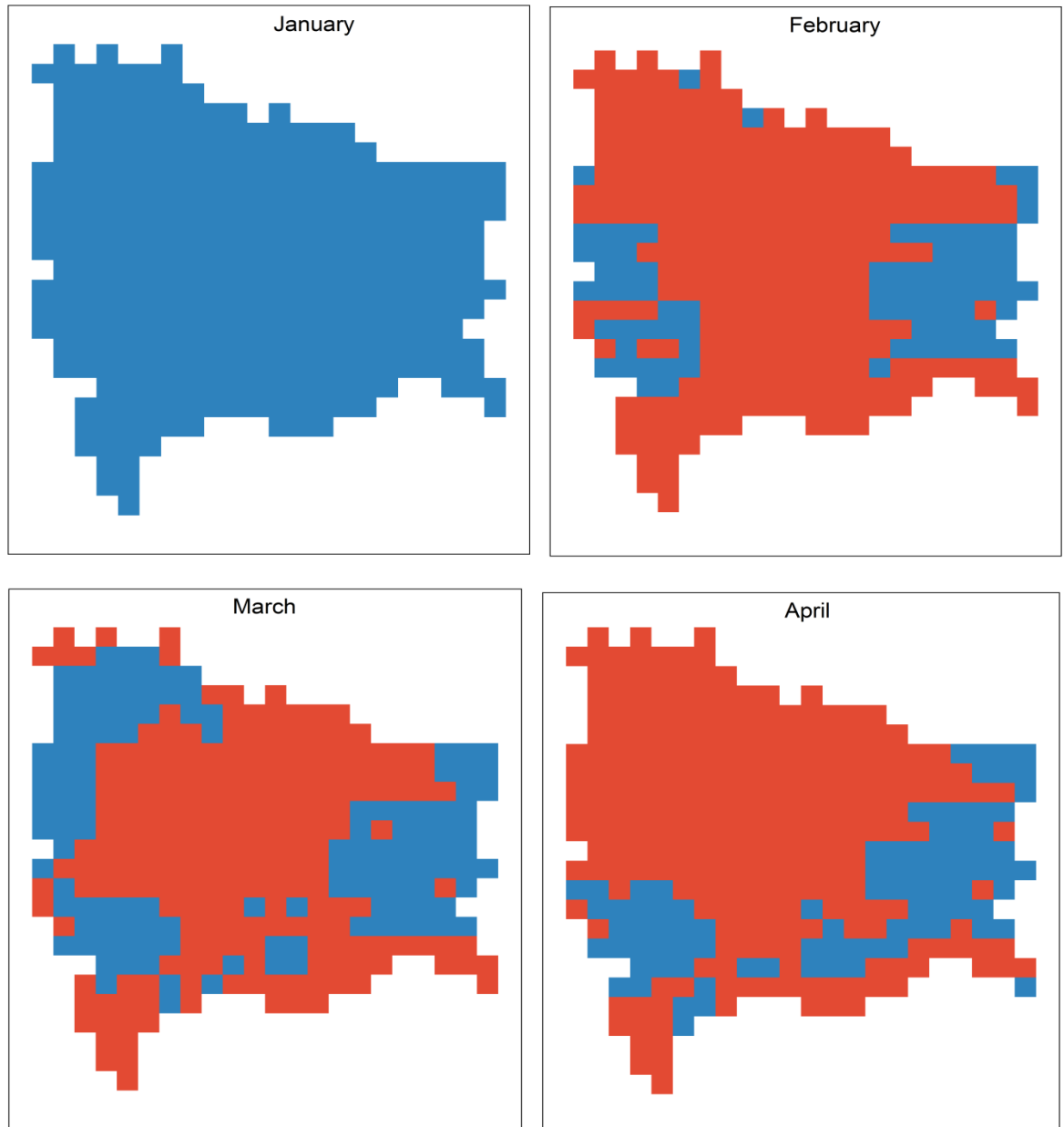
Figure 6: Month wise Box of Soil Moisture

There is a seasonal trend in the pattern of Soil Moisture for the 31 years monthly averaged value. Month of May exhibits the smallest range and also 25th and 75th percentile; however, the subsequent month (i.e. June) portrays just the contrasting observation.

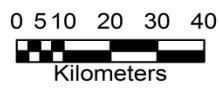
There occurs a distinct decreasing trend of Max, Min, 75th percentile, 25th percentile, Range and also the difference, 25 and 75 percentile SM values from January to May, and again, from October to December. The post-harvest/harvest month exhibits higher SM values than the winter and pre-monsoon months.

There occurs distinct difference/contrast between the two successive monsoon months (i.e., between June and July). The 75th percentile value of June is found to be lower than 25th percentile value of July.

Soil Moisture Trend Maps (1990-2020)



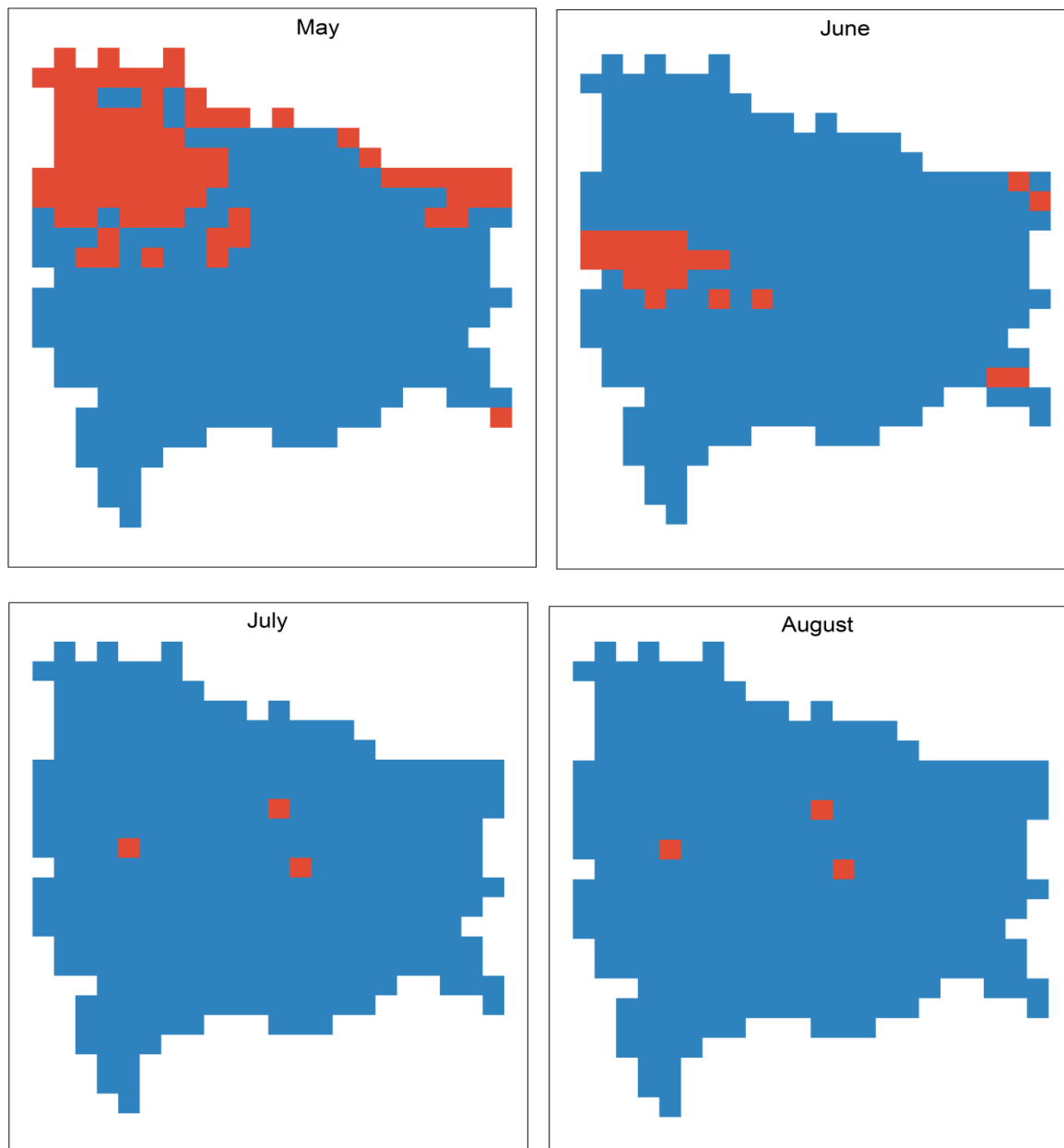
Increasing Decreasing No trend



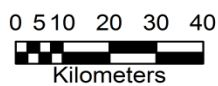
Source: Terra Climate

Figure 7: Soil Moisture Trend Map

Soil Moisture Trend Maps (1990-2020)



Increasing Decreasing No trend



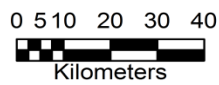
Source: Terra Climate

Figure 8: Soil Moisture Trend Map

Soil Moisture Trend Maps(1990-2020)



Increasing Decreasing No trend



Source: Terra Climate

Figure 9: Soil Moisture Trend Map

Month	Number of Pixels with Increasing Trend	Number of Pixels with Decreasing Trend	Number of Pixels Showing No Trend
January	0	0	337
February	0	258	79
March	0	210	127
April	0	249	88
May	0	81	256
June	0	22	315
July	0	307	30
August	0	3	334
September	1	0	336
October	0	221	116
November	0	19	318
December	0	0	337

Table 1 : Table showing the trend of Soil Moisture

No trend is observed in the month of January and December. Except the month of September which shows a increasing trend, January and December all other months show decreasing trend.

3.1.2 Precipitation

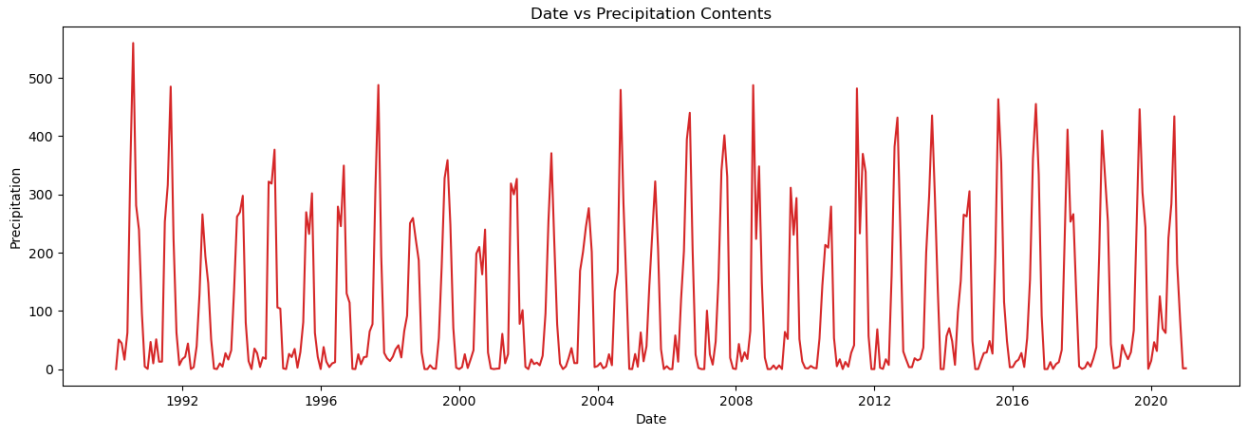


Figure 10: Precipitation Trend

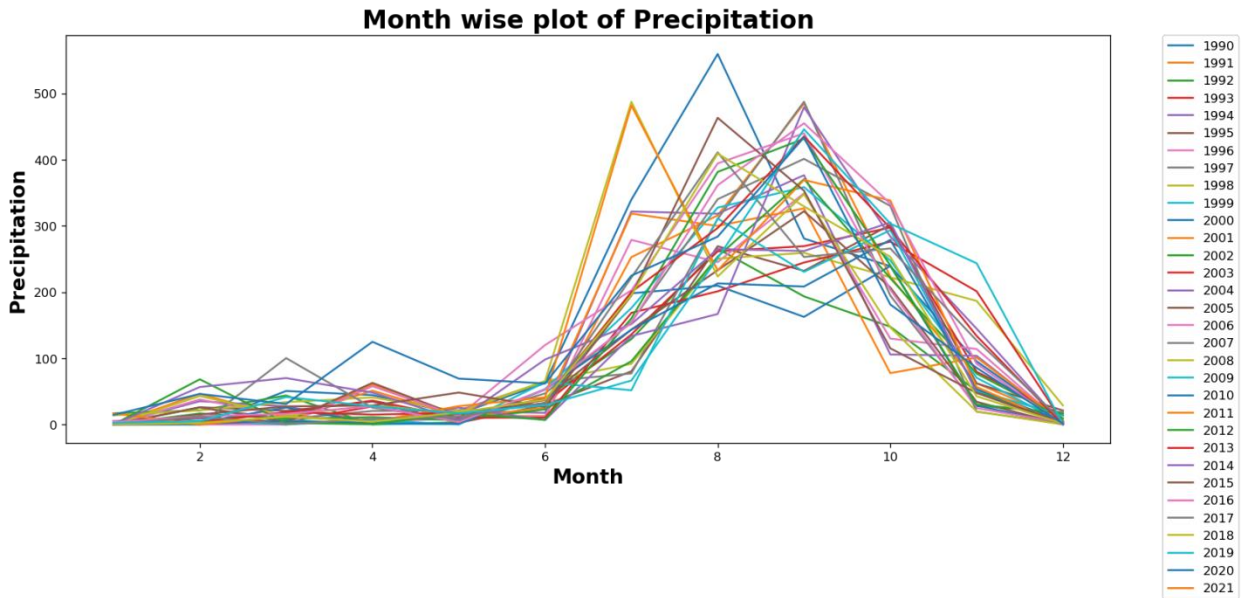


Figure 11: Month wise plot of Precipitation

**Year-wise Box Plot
(The Trend)**

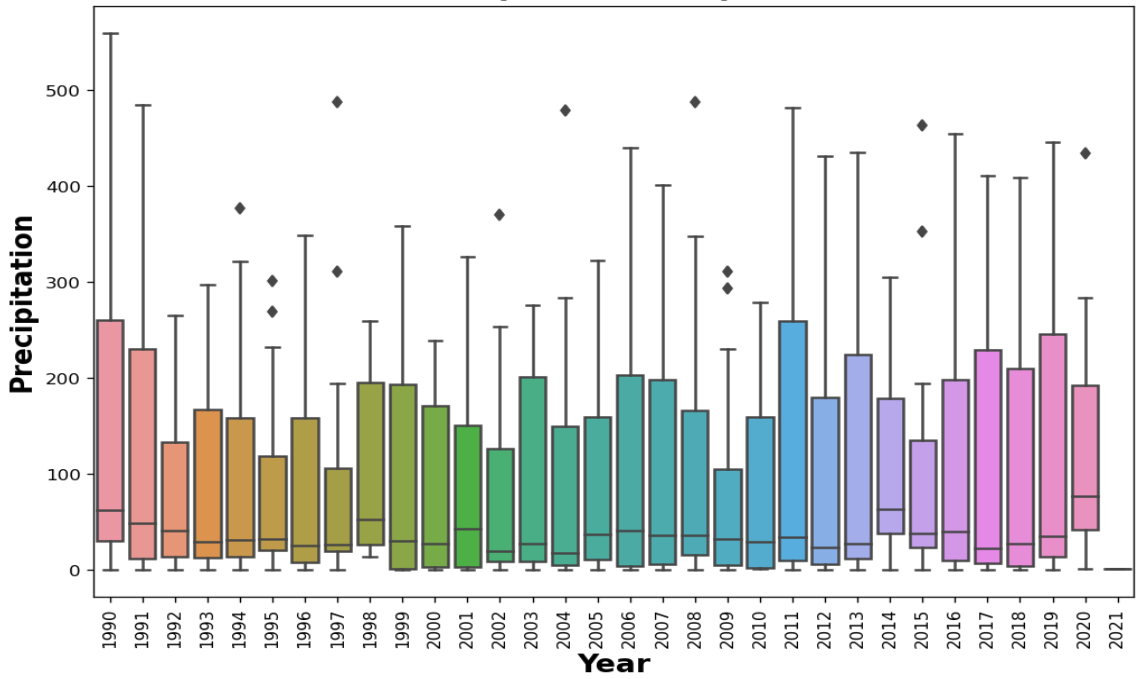


Figure 12: Year Wise Box Plot of Precipitation

Month-wise Box Plot

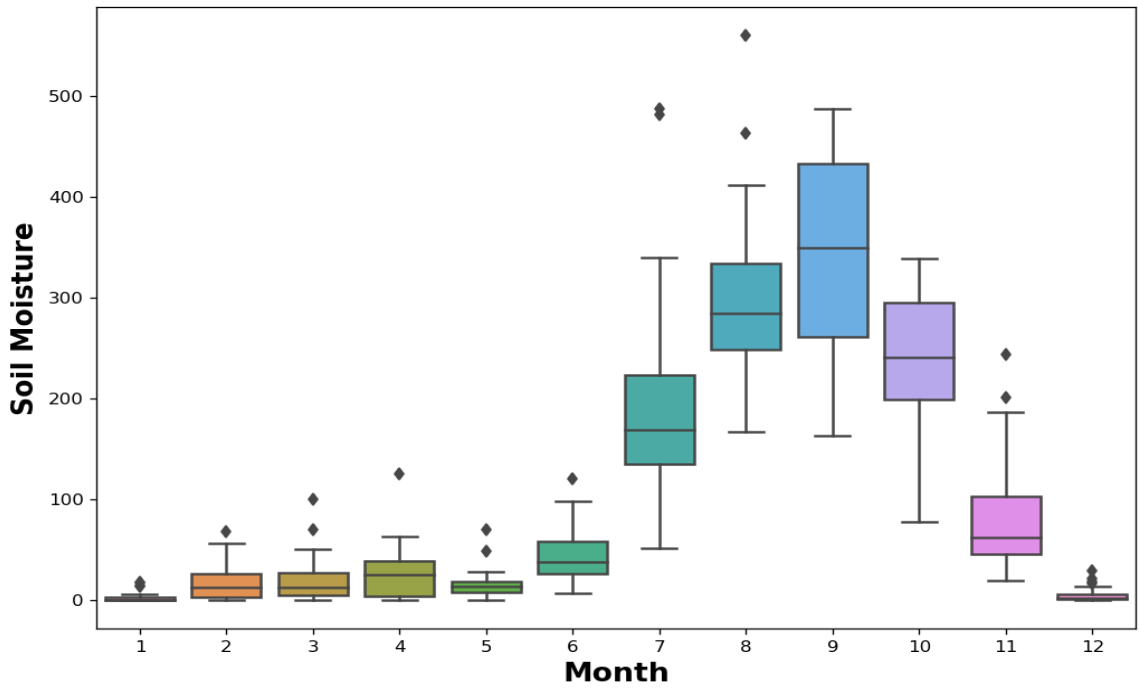
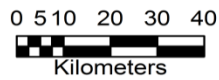
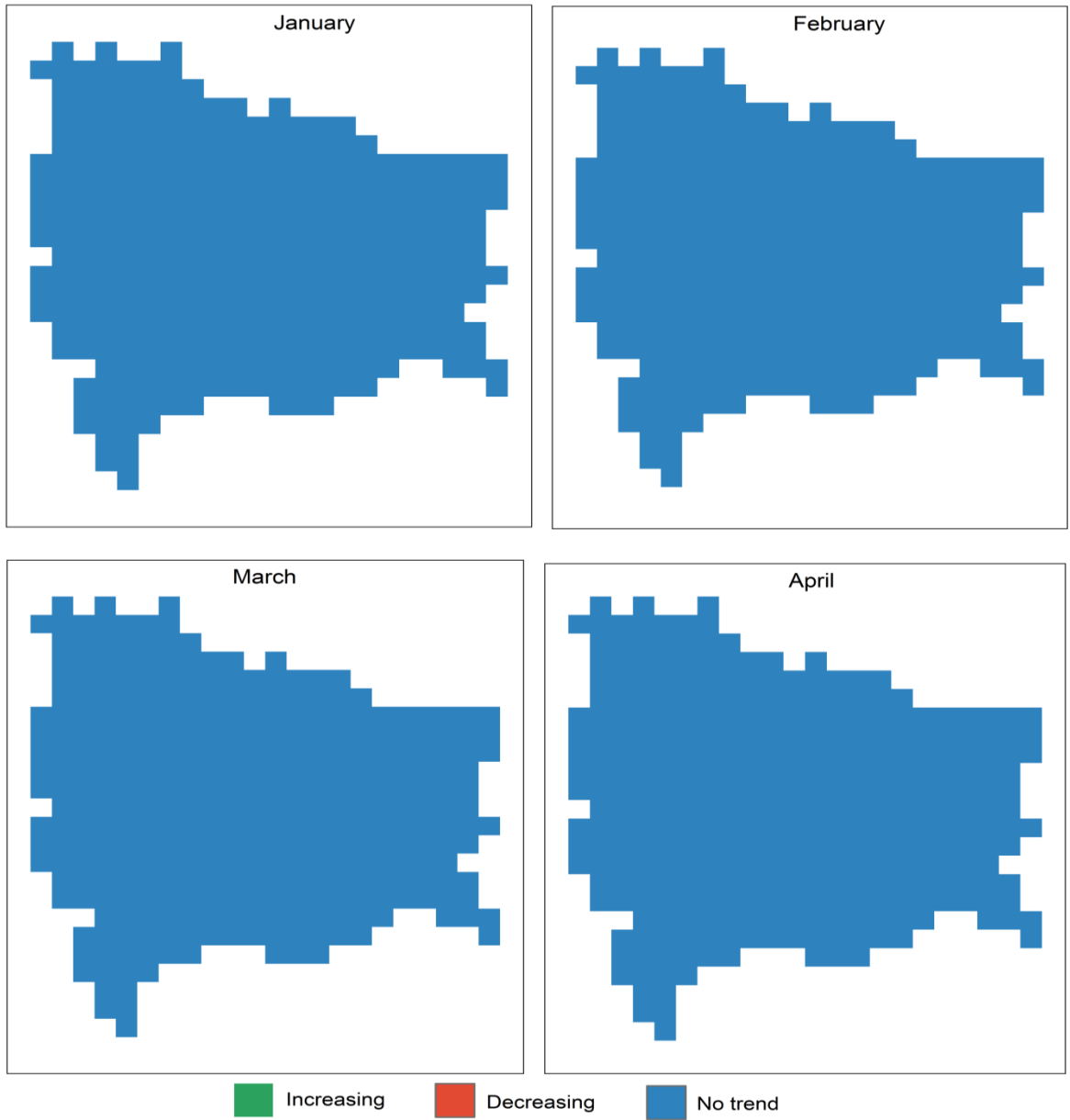


Figure 13: Month-wise Box plot for Precipitation

There exists a positive trend in precipitation from the month of June and it significantly rises to the maximum in the month of July, August and September in different years and starts decreasing by the month of November. The maximum precipitation is found in the years of 1990 and 2001 with values greater than 250mm. The median of all the years remains between 40mm and 60mm. Up to the year 1998 the lowest and 25 percentiles have significant gap but from the year 1999 to the year 2012 there exists similarity in the lowest value and 25 percentiles value.

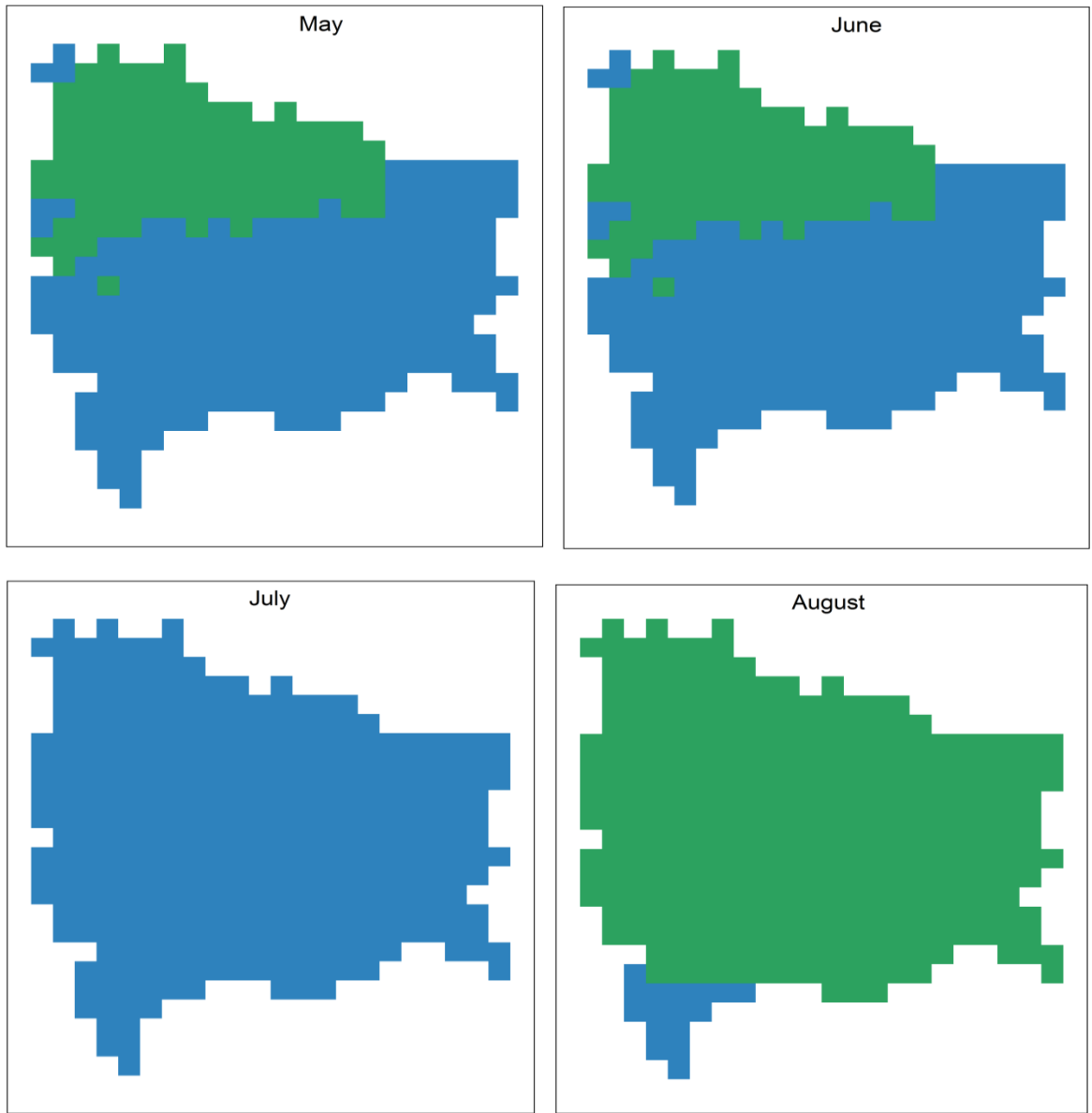
Precipitation Trend Maps(1990-2020)



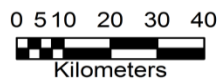
Source: Terra Climate

Figure 14: Precipitation Trend Map

Precipitation Trend Maps(1990-2020)



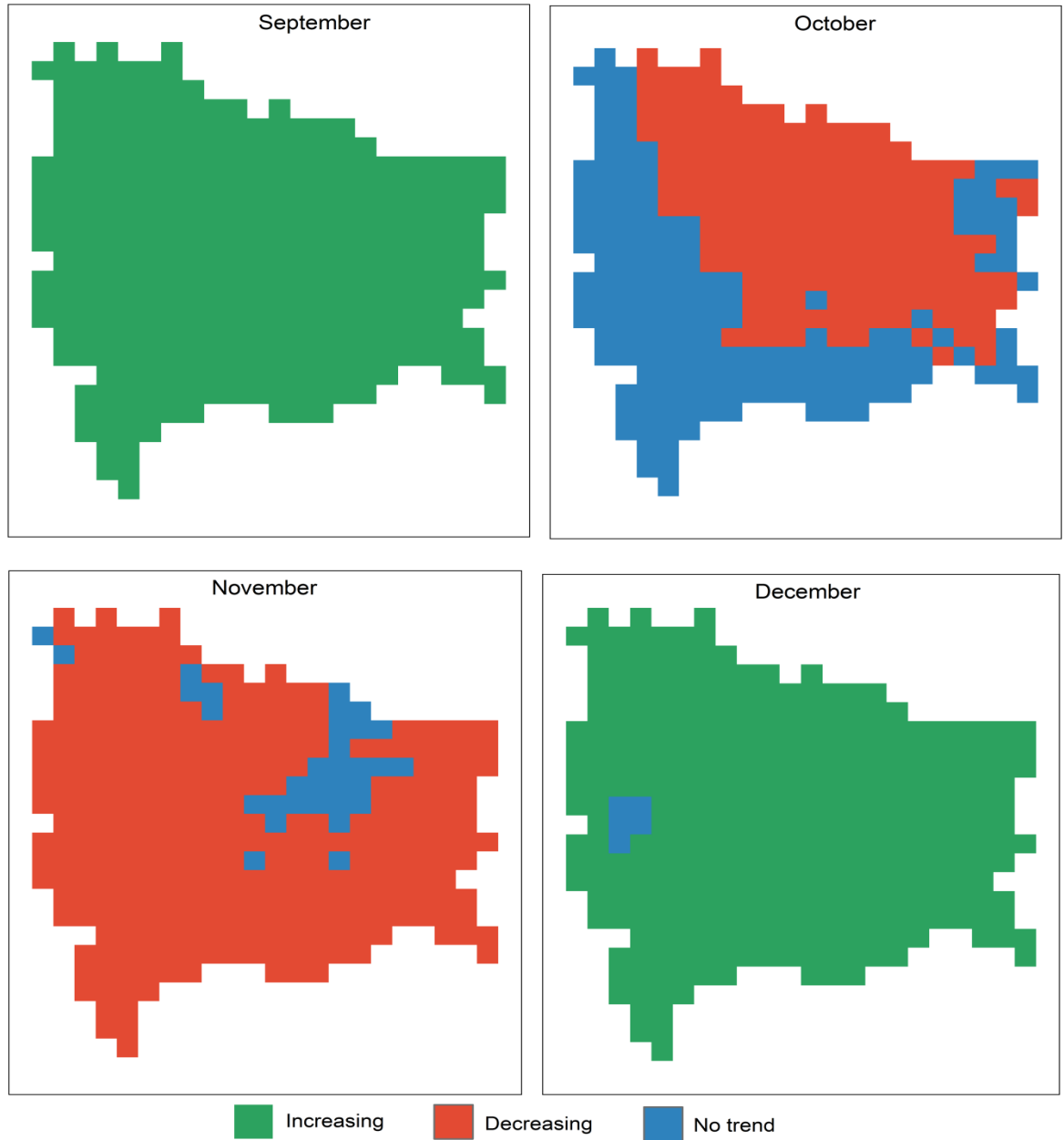
Increasing Decreasing No trend



Source: Terra Climate

Figure 15: Precipitation Trend Map

Precipitation Trend Maps(1990-2020)



0 5 10 20 30 40
Kilometers

Source: Terra Climate

Figure 16: Precipitation Trend Map

Month	Number of Pixels with Increasing Trend	Number of Pixels with Decreasing Trend	Number of Pixels Showing No Trend
January	0	0	337
February	0	0	337
March	0	0	337
April	0	0	337
May	48	0	289
June	48	0	289
July	0	0	337
August	321	0	16
September	0	0	337
October	0	0	337
November	0	189	148
December	332	0	5

Table 1: Table showing trends of precipitation

The months of May, June, August and December show increasing trend in some pixels thus signifying increase in rainfall. The month of November comprises a large number of pixels with decreasing trend signifying decrease in rainfall. The months January, February, March, April, July, September and October do not exhibit any trend.

3.1.3 Evapotranspiration

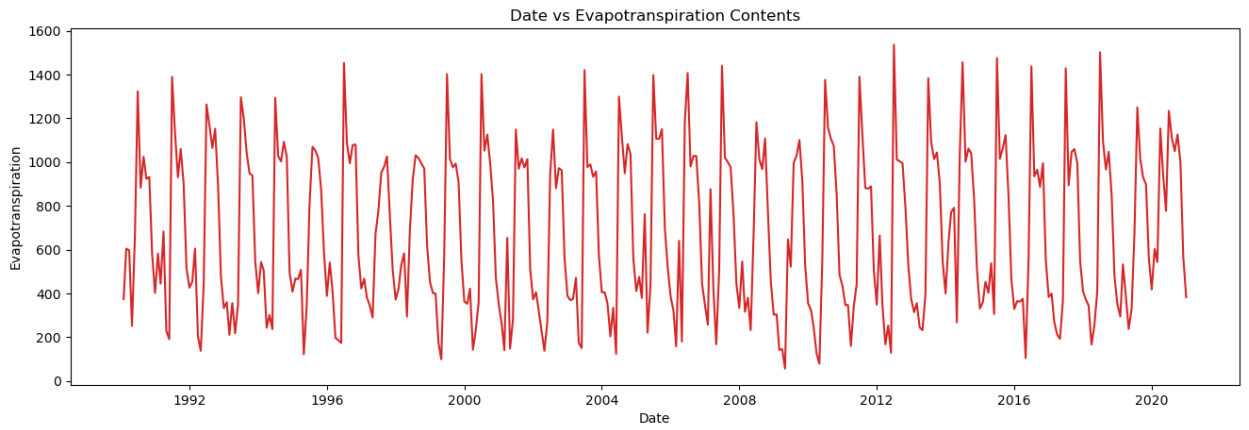


Figure 17: Trend of Evapotranspiration

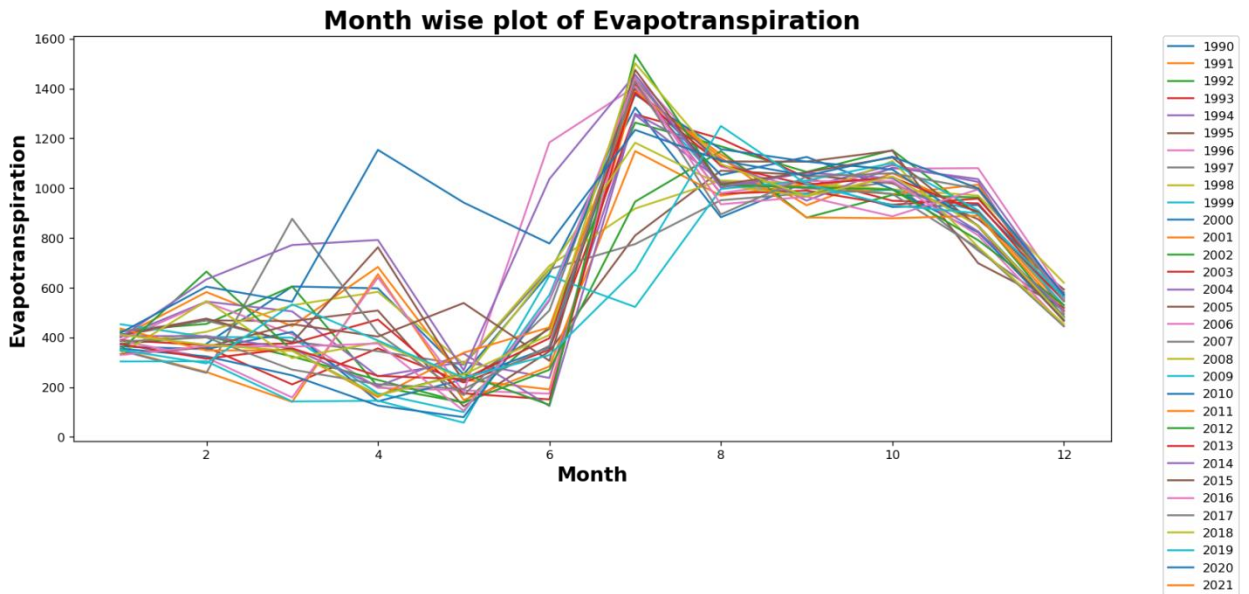


Figure 18: Month-wise trend of Evapotranspiration

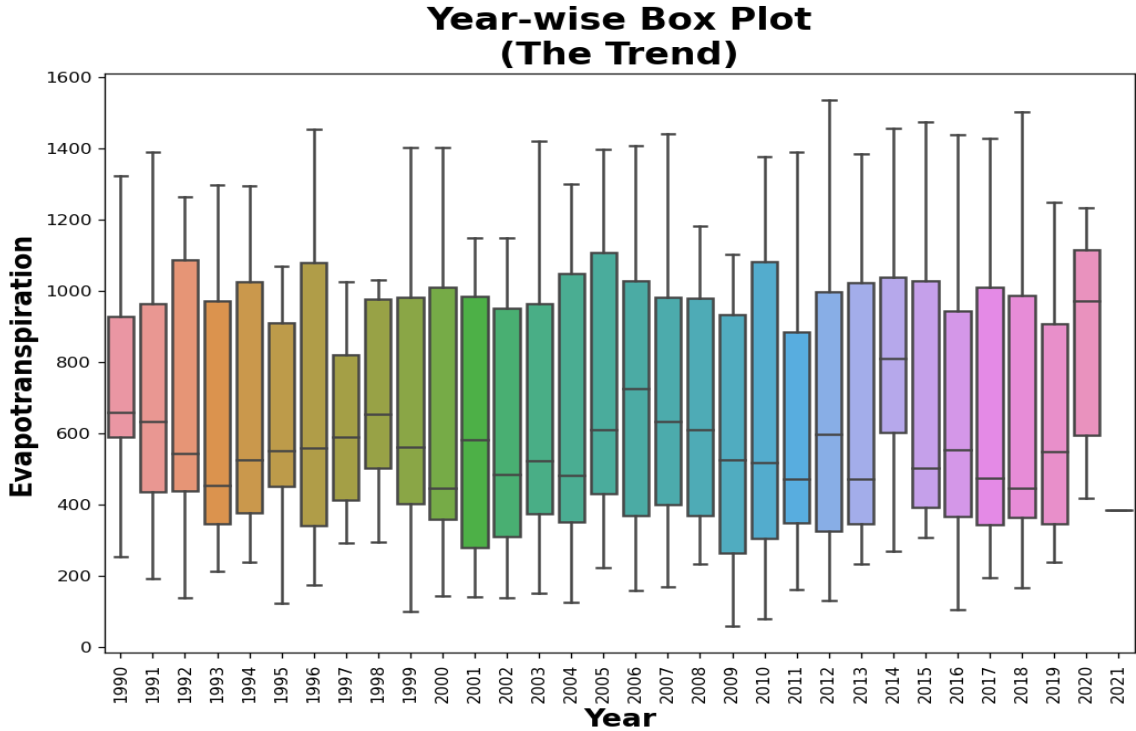


Figure 19: Year Wise Box Plot of Evapotranspiration

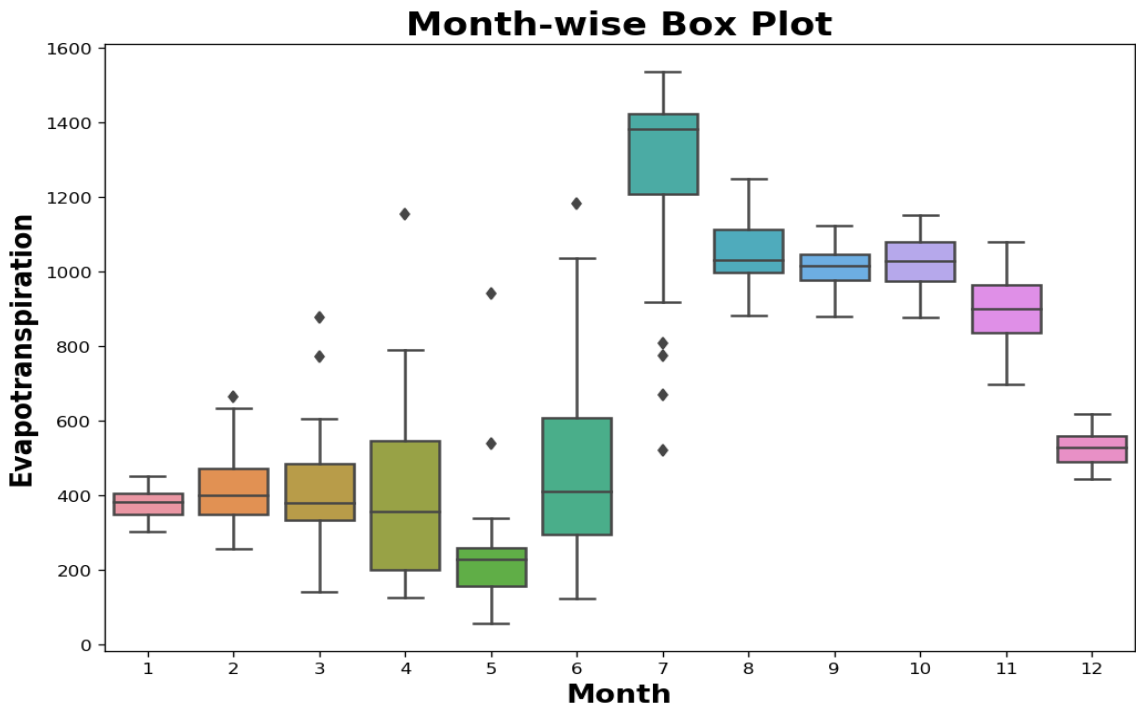
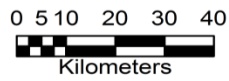
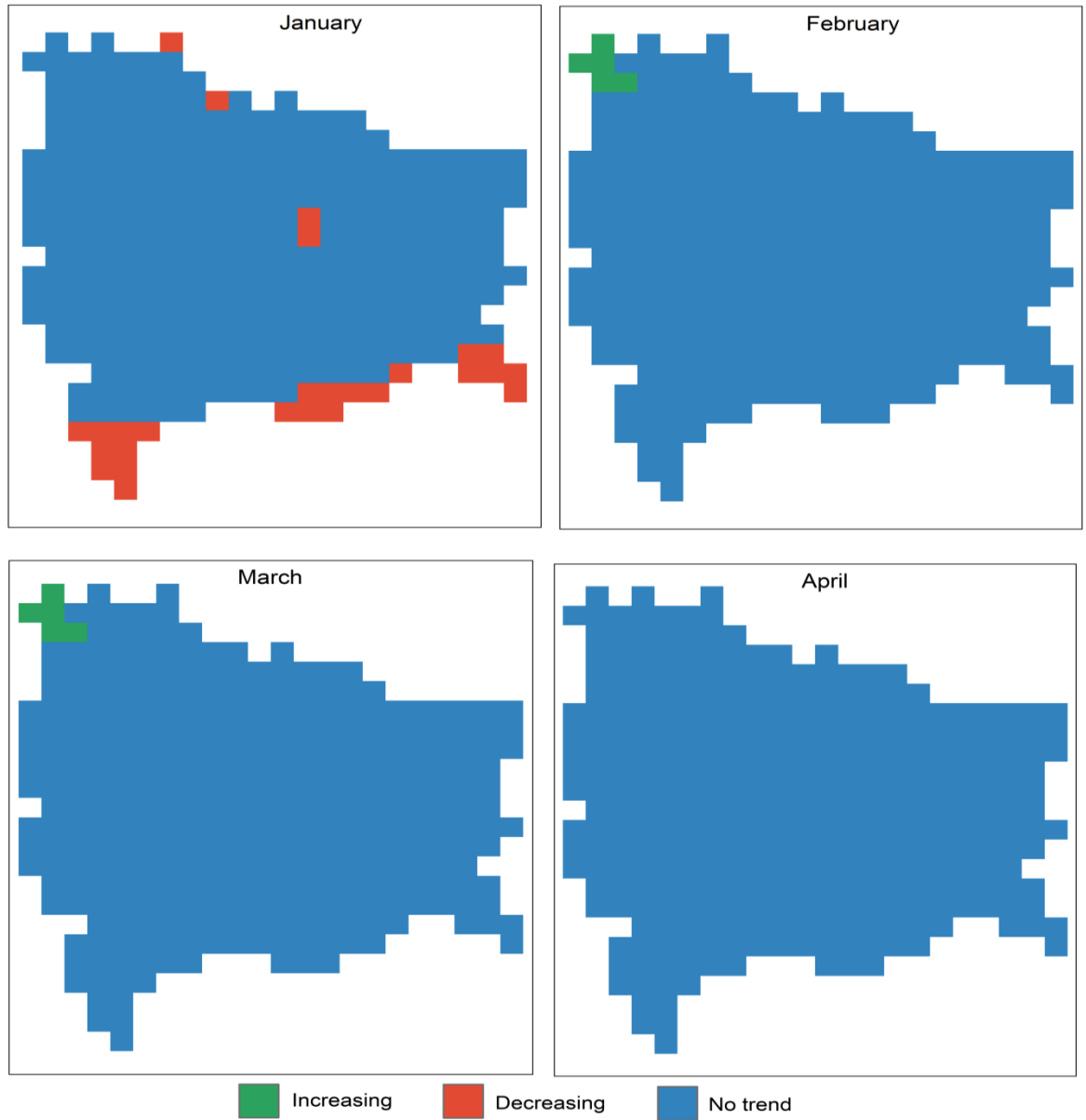


Figure 20: Month Wise Box Plot for Evapotranspiration

There exists a sharp increase of evapotranspiration from the month of June to July except in the years 1999, 2005 and 2006, which is followed by a sharp decline from August to October.

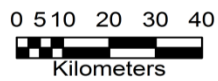
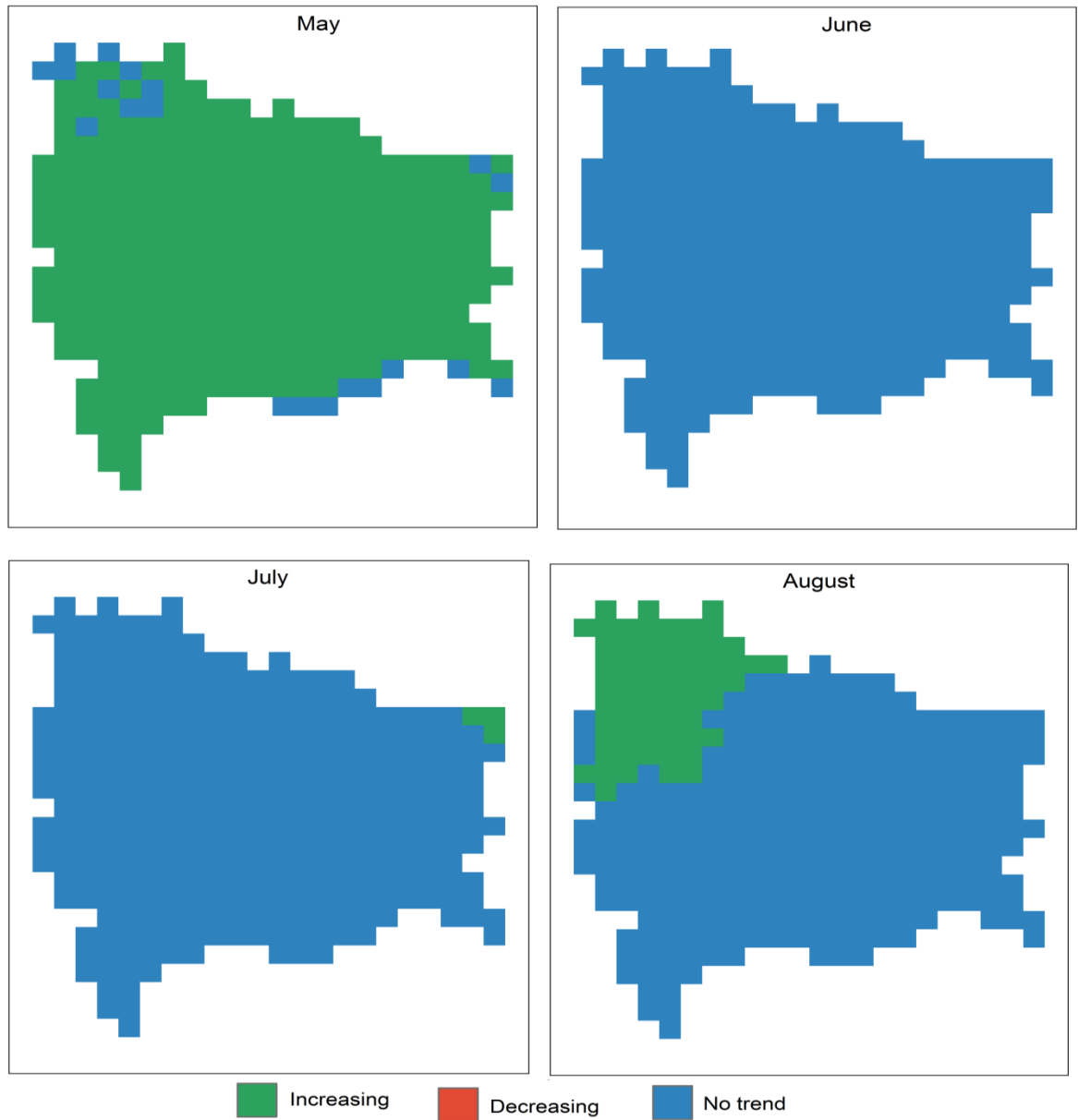
Evapotranspiration Trend Maps(1990-2020)



Source: Terra Climate

Figure 21: Evapotranspiration Trend Map

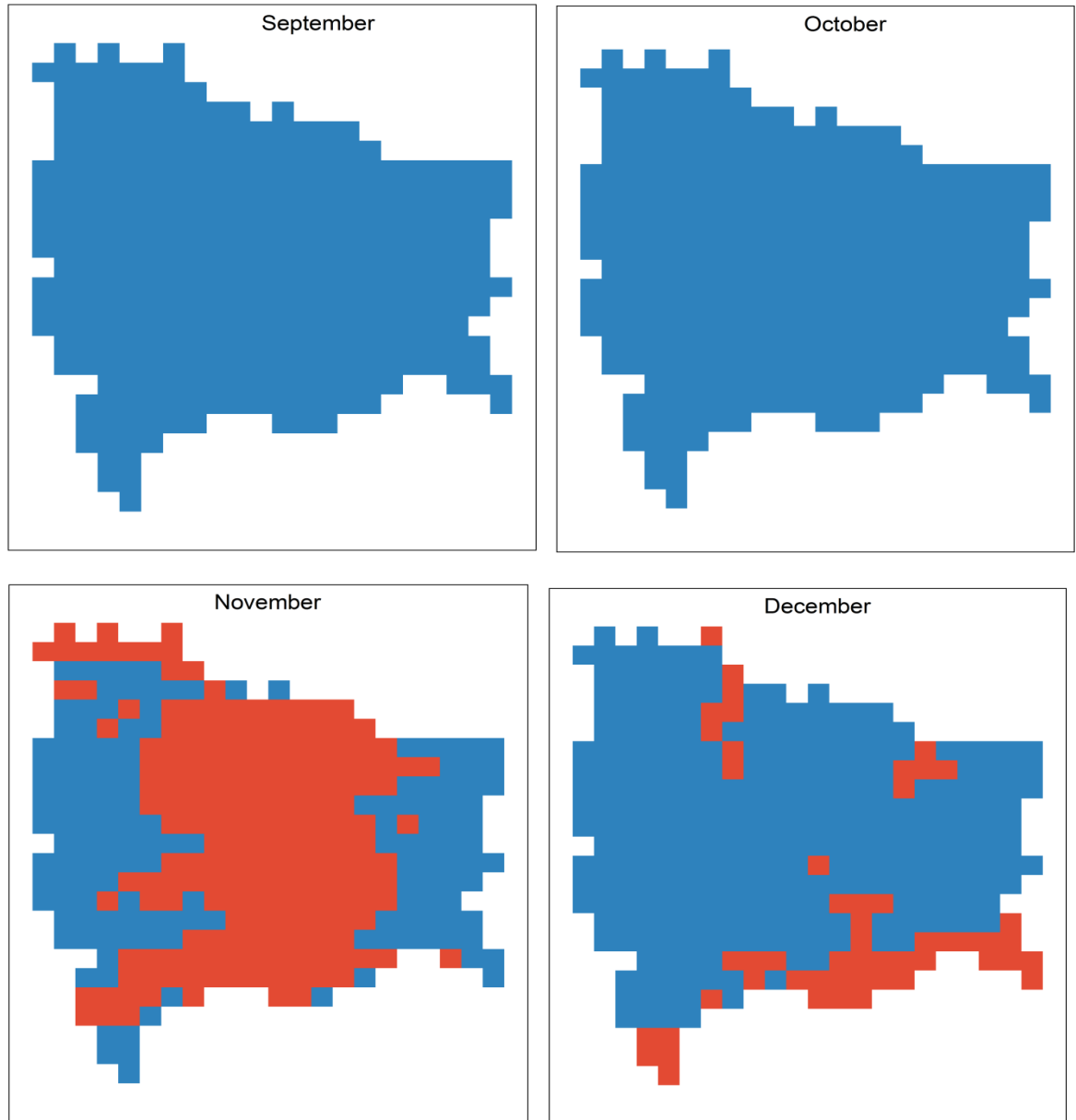
Evapotranspiration Trend Maps(1990-2020)



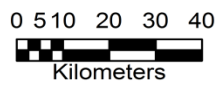
Source: Terra Climate

Figure 22: Evapotranspiration Trend Map

Evapotranspiration Trend Maps(1990-2020)



Increasing Decreasing No trend



Source: Terra Climate

Figure 23: Evapotranspiration Trend Map

Month	Number of Pixels with Increasing Trend	Number of Pixels with Decreasing Trend	Number of Pixels Showing No Trend
January	27	0	310
February	5	0	332
March	5	0	332
April	0	0	337
May	317	0	20
June	0	0	337
July	3	0	334
August	61	0	276
September	0	0	337
October	0	0	337
November	0	189	148
December	0	53	284

Table - 3 : Trend Table for Evapotranspiration

The months April, June, September and October shows no change in the trend in the entire study area. The month January, February, March and August shows increase in the level of evapotranspiration and the month of May shows 317 pixels i.e. 94% of the pixels shows a increment in the trend of Evapotranspiration. Month of November and December show a decrease in the trend of Evapotranspiration.

3.1.4 Highest Temperature

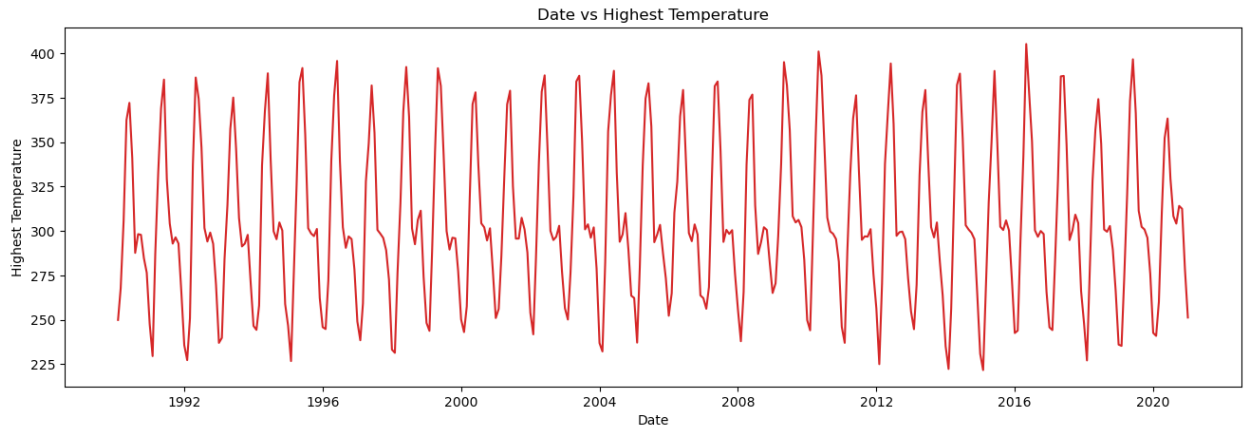


Figure 24: Highest Temperature Trend

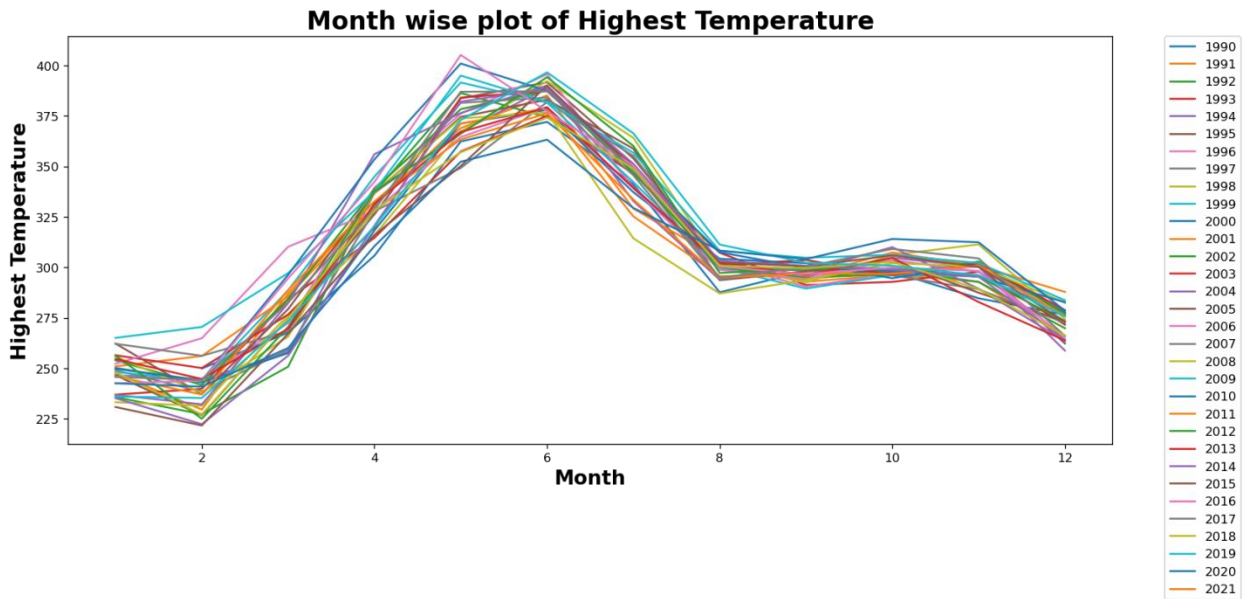


Figure 25: Month Wise Plot of Highest Temperature
(Conversion Factor for Temperature is 0.1°C)

**Year-wise Box Plot
(The Trend)**

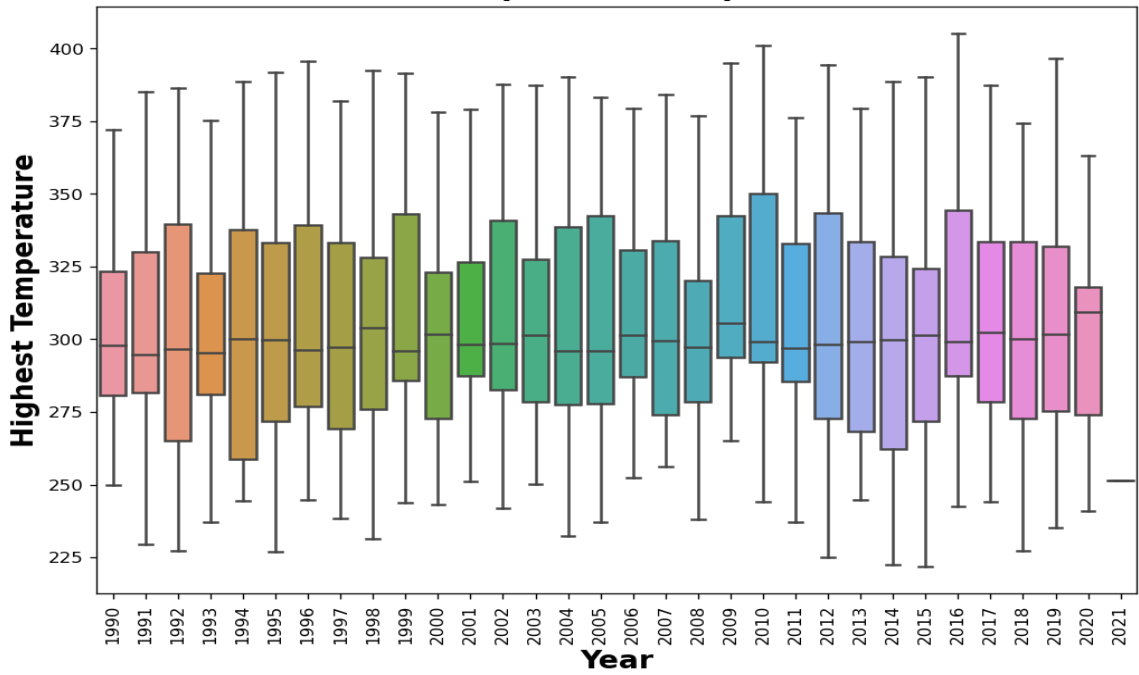


Figure 26: Year Wise Box Plot for Highest Temperature

Month-wise Box Plot

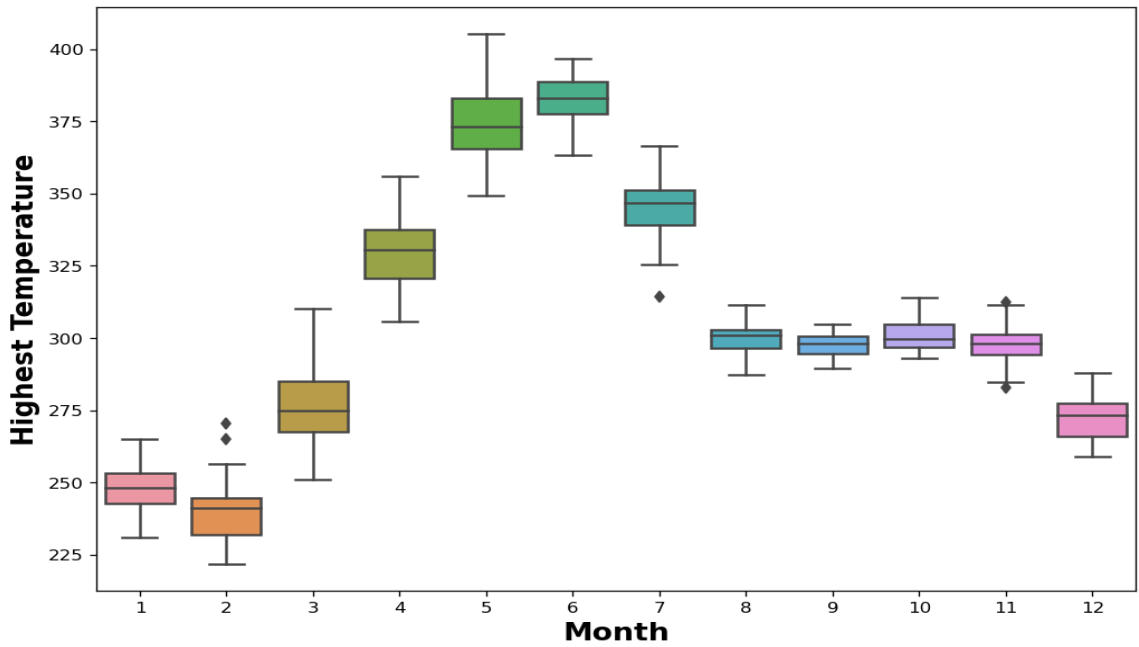
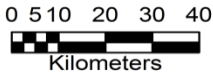
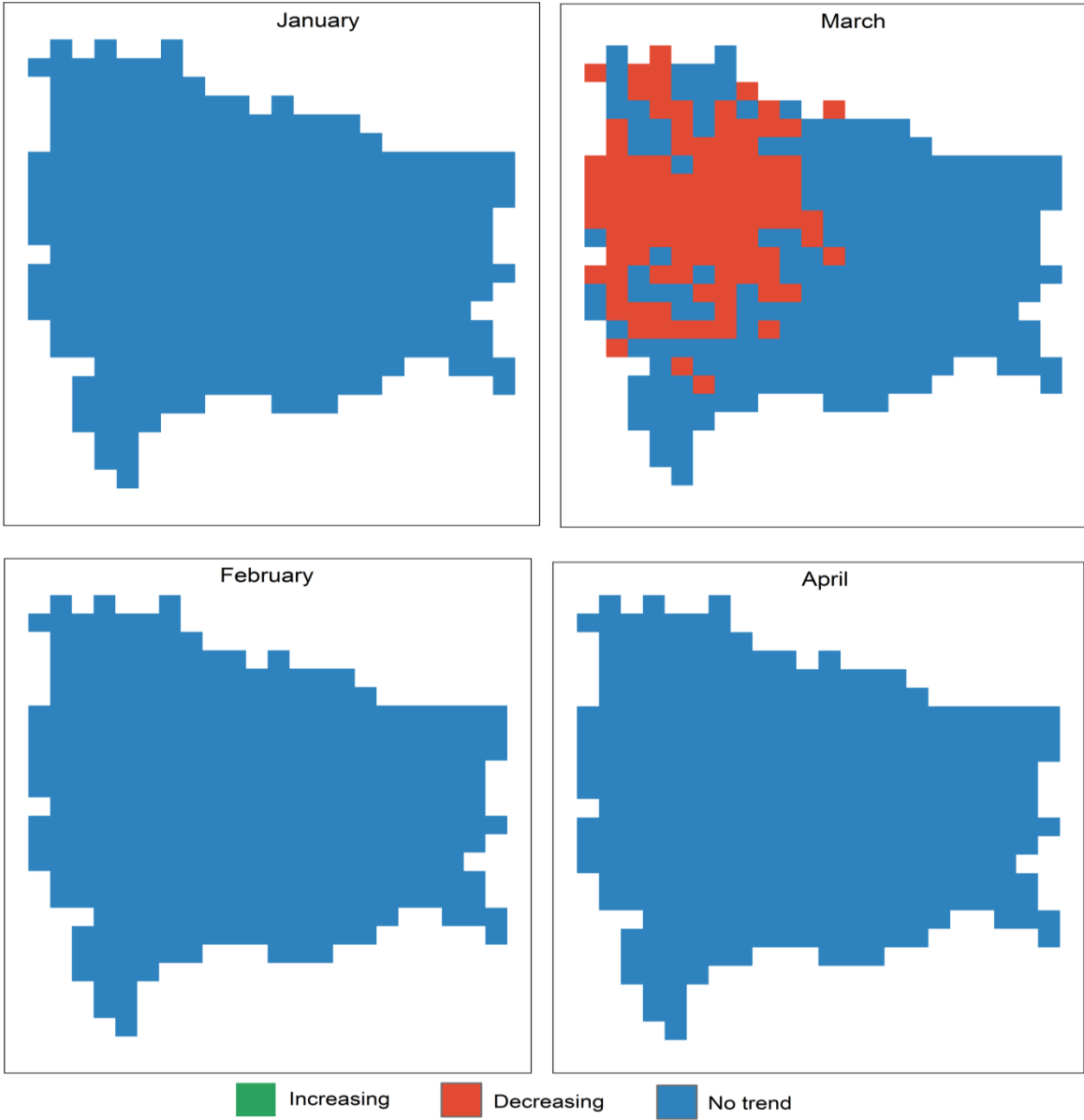


Figure 27: Month-wise Box Plot for Highest Temperature

The highest temperature shows a seasonal variation. There is a uniform increase in the highest temperature from February to June after which the trend starts to fall and halts in the month of August and there is a low level fall of the highest temperature. From the Year-wise box-plot we can come to know there is a lowly varying median value nearing about 30°C.

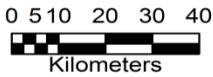
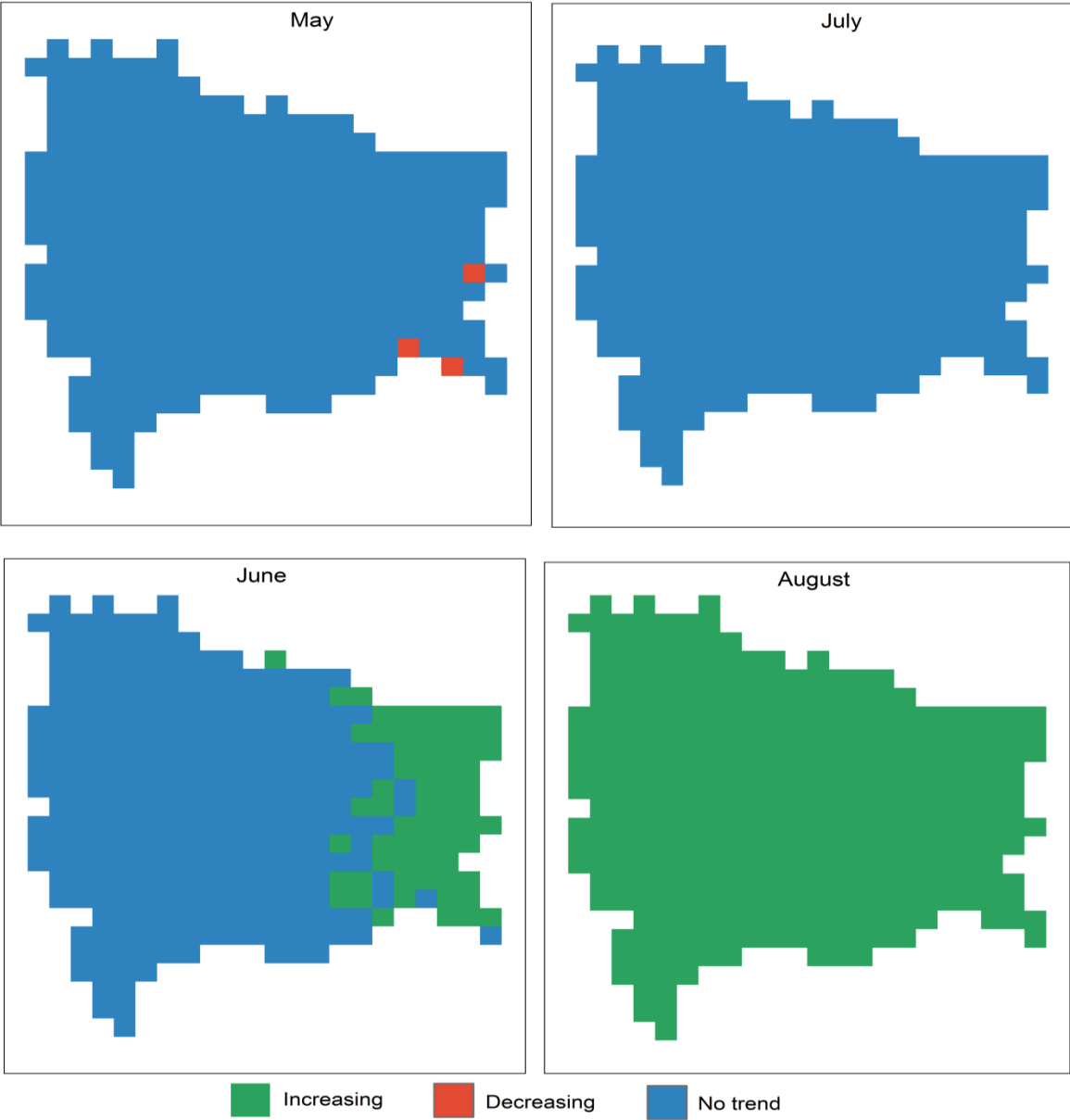
Highest Temperature Trend Maps (1990-2020)



Source: Terra Climate

Figure 28: Highest Temperature Trend Map

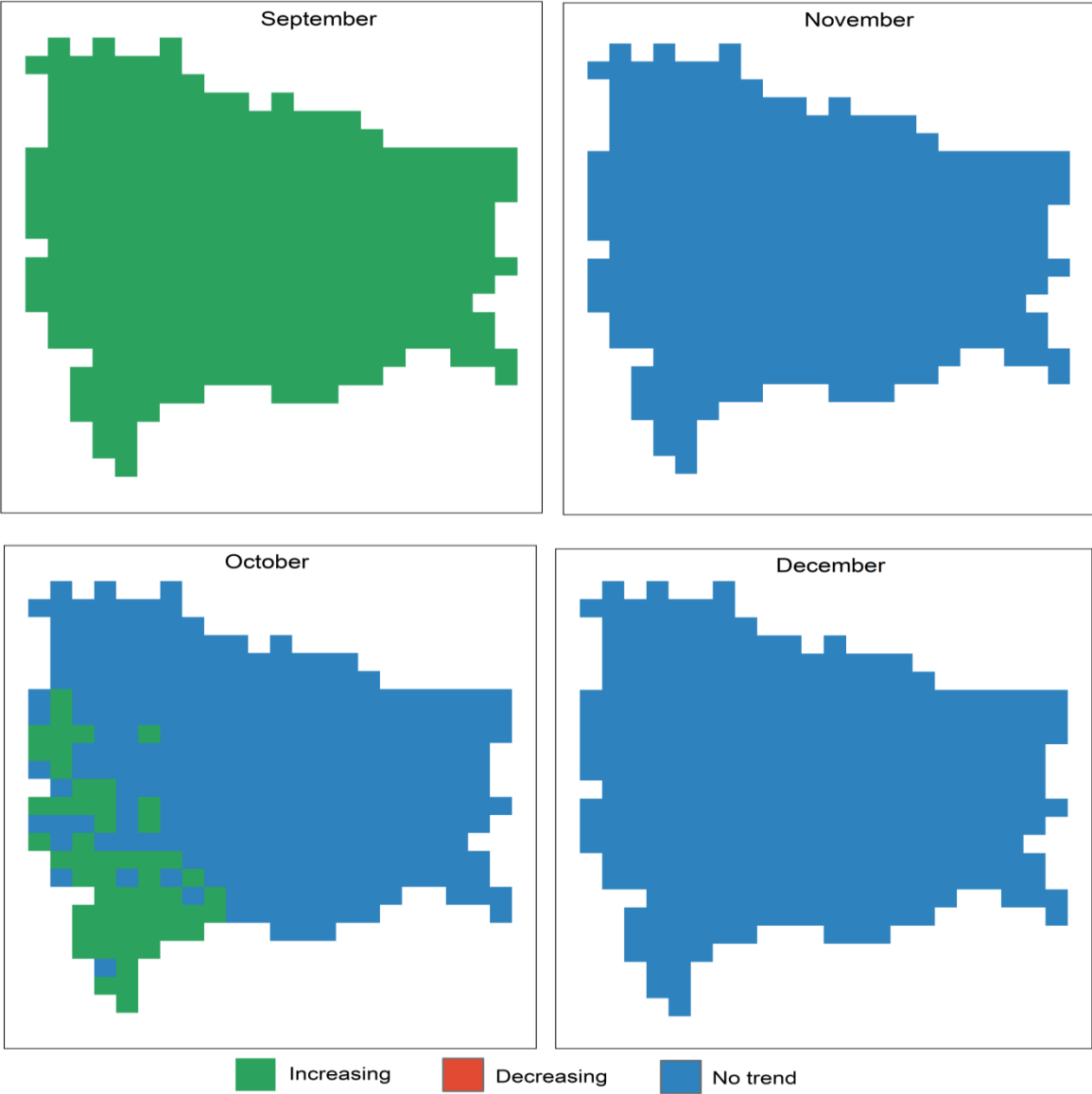
Highest Temperature Trend Maps (1990-2020)



Source: Terra Climate

Figure 29: Highest Temperature Trend Map

Highest Temperature Trend Maps (1990-2020)



Source: Terra Climate

Figure 30: Highest Temperature Trend Map

Month	Number of Pixels with Increasing Trend	Number of Pixels with Decreasing Trend	Number of Pixels Showing No Trend
January	0	0	337
February	0	104	238
March	0	0	337
April	0	0	337
May	0	3	334
June	0	64	273
July	0	0	334
August	0	0	337
September	0	0	337
October	56	0	281
November	0	0	337
December	0	0	337

Table-4 : Trend Table for Highest Temperature

The months of January, March, April, July, August, September, November and December shows no sign in the change of trend in the highest temperature for the 31 years in the study area. The month of October shows an increasing trend for 56 pixels. February and June show the decreasing trend.

3.1.5 Minimum Temperature

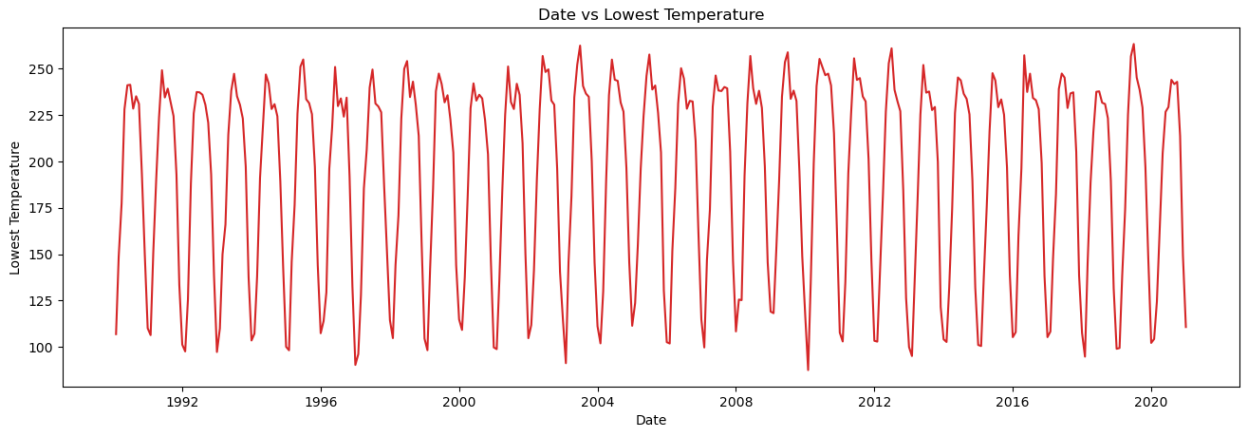


Figure 31: Lowest Temperature Trend

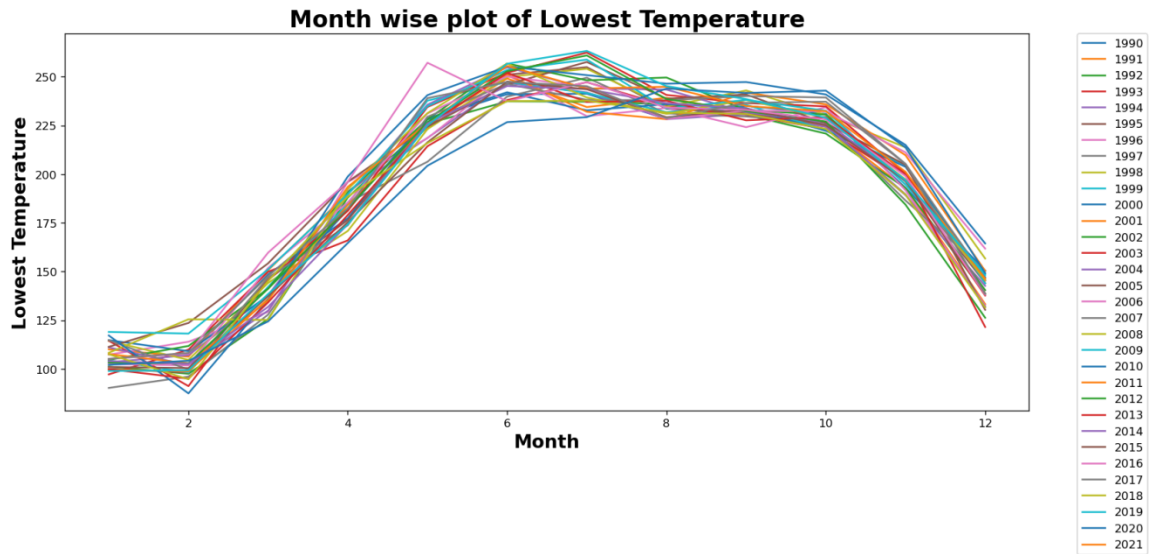


Figure 32: Month Wise plot for Lowest Temperature
(Conversion Factor for Temperature is 0.1°C)

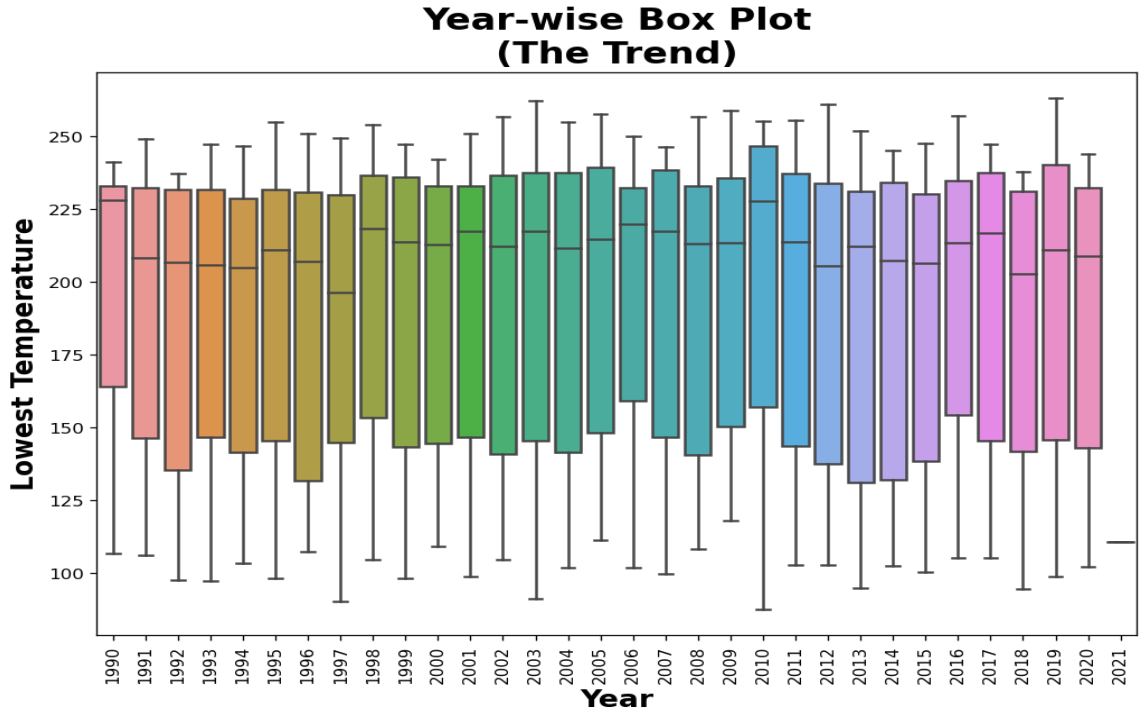


Figure 33: Year Wise Box plot for Lowest Temperature

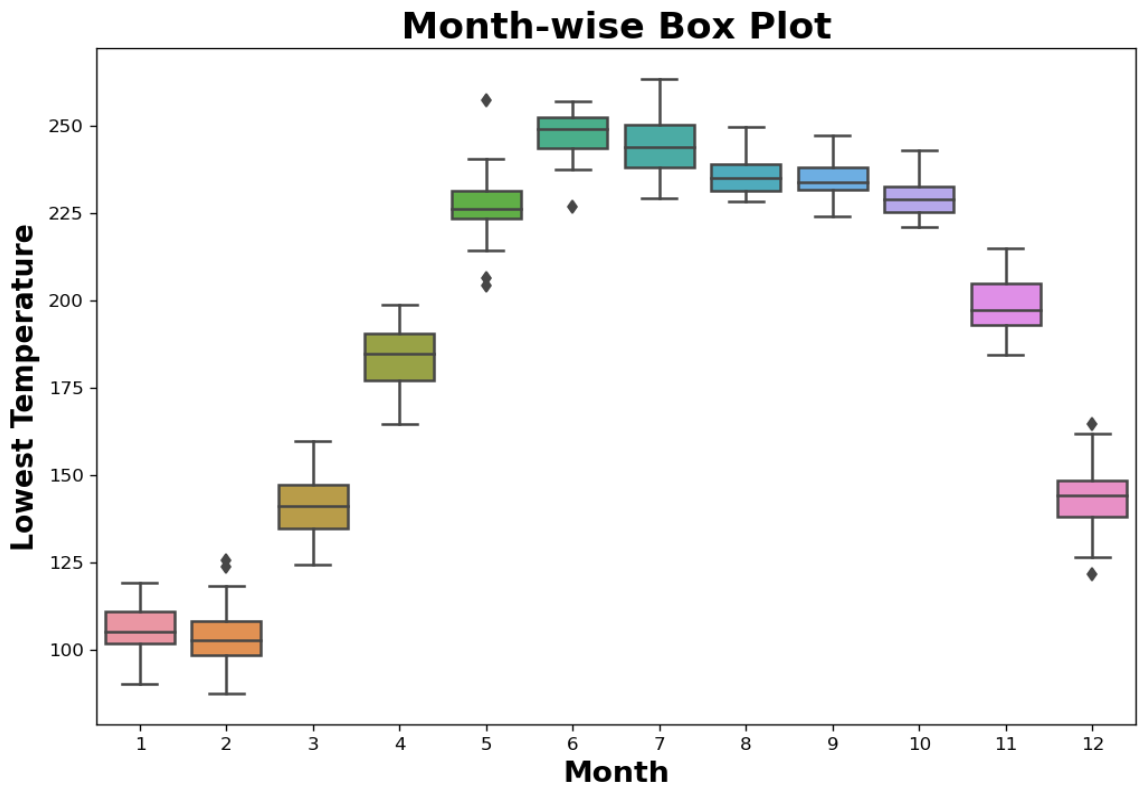
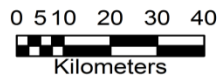
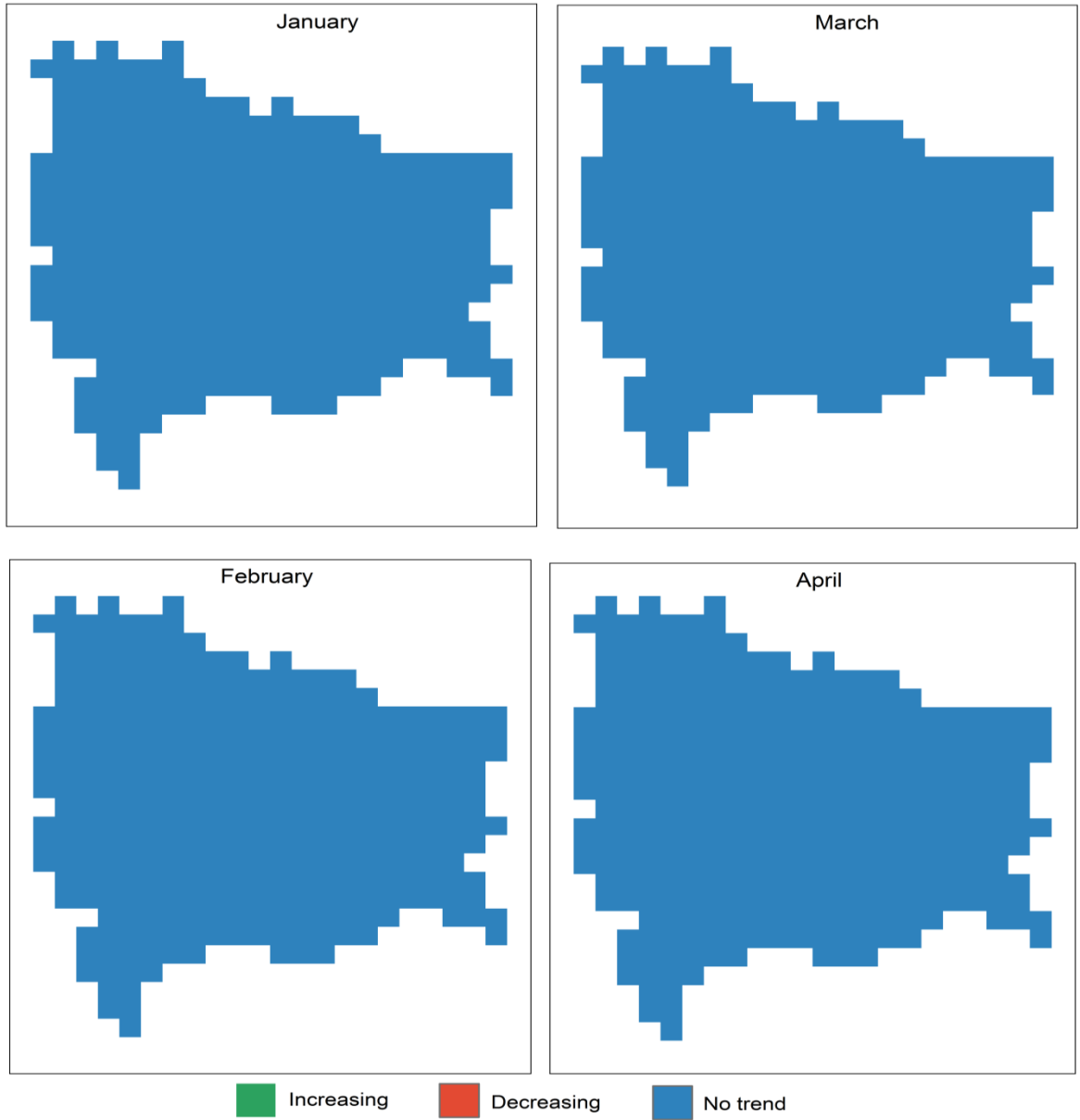


Figure 34: Month wise Box Plot for Lowest Temperature

There is a uniform increase in the lowest temperature from February to June after which the trend starts to fall and halts in the month of August and there is a low level fall of the lowest temperature. From the Year-wise boxplot we can come to know there is a lowly varying median value nearing about 30°C.

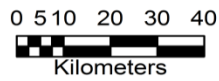
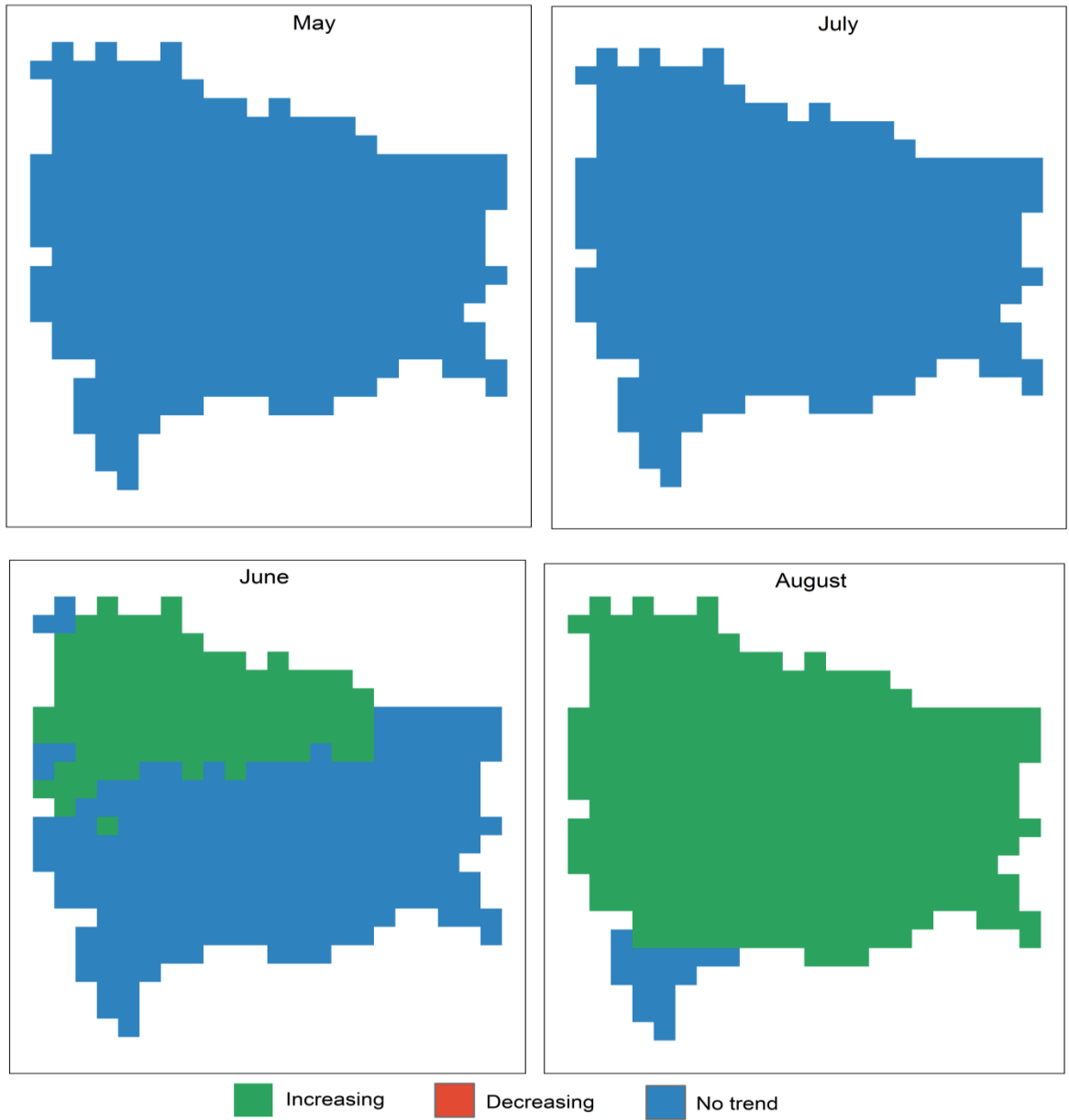
Lowest Temperature Trend Maps (1990-2020)



Source: Terra Climate

Figure 35: Lowest Temperature Trend Map

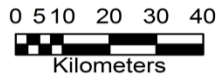
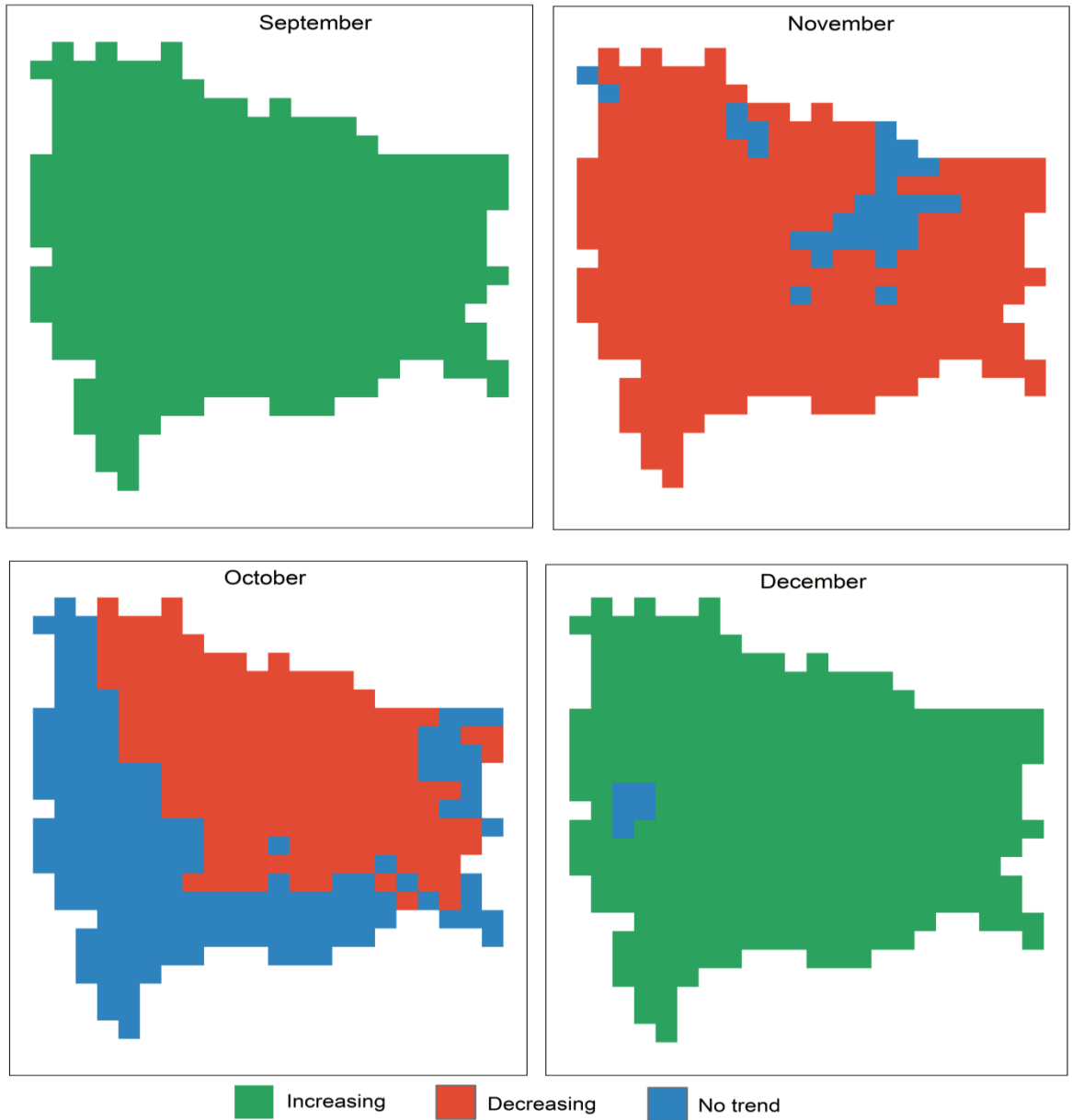
Lowest Temperature Trend Maps (1990-2020)



Source: Terra Climate

Figure 36: Lowest Temperature Trend Map

Lowest Temperature Trend Maps (1990-2020)



Source: Terra Climate

Figure 37: Lowest Temperature Trend Map

Month	Number of Pixels with Increasing Trend	Number of Pixels with Decreasing Trend	Number of Pixels Showing No Trend
January	0	0	337
February	0	0	337
March	0	0	337
April	0	0	337
May	0	0	337
June	109	0	228
July	0	0	337
August	321	0	16
September	0	0	337
October	0	175	162
November	0	305	32
December	332	0	5

Table 5: Trend Table for Lowest Temperature

The months of January, February, March, April, May and September shows no change in the trend of Lowest Temperature. June, August and December shows a increasing trend where August and December shows a 95% and 98% of the pixels to follow the increasing trend. October and November shows decreasing trend for the study area.

Chapter Four

4.1 Conclusion

An important aspect of study for trend in Soil Moisture, Precipitation, Evapotranspiration, Highest and Lowest Temperature has been carried out for the district of Ranchi and Khunti of Jharkhand, India.

- It is observed that there is a decrease in the trend of monthly soil moisture in the 31 years for a large extent.
- In case of precipitation in January to April no trend was observed rest there was increasing in the monthly 31 year for a big extent.
- In evapotranspiration there is a increase from the month of Late May to June and follows the trend of precipitation.
- For the highest temperature we find a constant increase of trend in the month of August and September for the last 31 years.
- In lowest temperature we also find similar trend as the highest temperature showing a hike in temperature which can be well suited accordance to climate change.

Reference

- Angström, a. "the albedo of various surfaces of ground". *Geogr. Ann.*,7, 323–327,1925
- Abatzoglou, j.t., s.z. Dobrowski, s.a. Parks, k.c. Hegewisch, 2018, terraclimate, a high-resolution global dataset of monthly climate and climatic water balance from 1958-2015, scientific data 5:170191, [doi:10.1038/sdata.2017.191](https://doi.org/10.1038/sdata.2017.191).
- Astm d 4642-87, "standard test method for determination of water moisture content of soil by the microwave oven method ", 1987.
- Bach, h.; mauser, w. "modelling and model verification of the spectral reflectance of soils under varying moisture conditions".in proceedings of the international geoscience and remote sensing symposium, 1994. Igarss '94. Surface and atmospheric remote sensing: technologies, data analysis and interpretation, pasadena, ca, usa, volume 4, pp. 2354–2356, 1994.
- E. e. abdel-hady, a.m.a..el-sayed and h.b.aiaa , "determination of moisture content and natural radioactivity in soils using gamma spectroscopy", third radiation pkytk* conf* auminia, 13 -17 nov 1996.
- K. Grote, s. Hubbard, y. Rubin , "field-scale estimation of volumetric water content using ground penetrating radar ground wave techniques", water resources research, vol. 39, no. 11, 1321, 2003.
- Michael l.whiting, lin li, susan l. Ustin, "predicting water content using gaussian model on soil spectra", remote sensing of environment 89, 535–552,2004.
- Mann, h.b. (1945) non-parametric tests against trend. *Econometrica*, 13, 163–171.
- J.a.m. Demattê , antonio a. Sousa marcelo c.alves , marcos r. Nanni ,peterson r. Fiorio, rogerio costa campos , "determining soil water status and other soil
- Willem w. Verstraeten1,* , frank veroustraete 2 and jan feyen , "assessment of evapotranspiration and soil moisture content across different scales of observation",sensors, 8, 70-117, 2008.
- Haubrock, s.; chabrillat, s.; lemmnitz, c.; kaufmann, h., "surface soil moisture quantification models from reflectance data under field conditions". *Int. J. Remote sens.* 29, 3–29,2008.
- Soren-nils haubrock" , sabine chabrillat, matthias kuhnert, patrick hostert and hermann kaufmann , "surface soil moisture quantification and validation based on hyperspectral data and field measurements", journal of applied remote sensing, vol. 2, 023552 , 2008.

Michael I. Whiting, “measuring surface water in soil with light reflectance”, *proc. Of spie* vol. 7454 74540d-1 ,2009

Heyam daod , “determination of moisture content and liquid limit of foundations soils, using microwave radiation, in the different locations of sulaimani governorate, kurdistan region-iraq”,*international journal of civil, environmental, structural, construction and architectural engineering* vol:6, no:7, 2012

Susha lekshmi s.u. , d.n. Singh , maryam shojaei baghini , “a critical review of soil moisture measurement ”, *s.l. S.u. Et al. / measurement* 54 ,92–105, 2014.

Attila nagy ,péterriczu, bernadettgálya, jánostamás , “spectral estimation of soil water content in visible and near infrared range”, *eurasian journal of soil science* 3 ,163 – 171, 2014.

Sophie fabre , xavier briottet and audrey lesaignoux , “estimation of soil moisture content from the spectral reflectance of bare soils in the 0.4–2.5 μm domain”, *sensors*, 15, 3262-3281,2015.

Xie, Y., Liu, S., Huang, S., Fang, H., Ding, M., Huang, C., & Shen, T. (2022). Local trend analysis method of hydrological time series based on piecewise linear representation and hypothesis test. *Journal of Cleaner Production*, 339, 130695.

Mann, H. B. (1945). Nonparametric Tests Against Trend. *Econometrica*, 13(3), 245. doi:10.2307/1907187

Şen, Z. (2017). Hydrological trend analysis with innovative and over-whitening procedures. *Hydrological Sciences Journal*, 62(2), 294-305.

Hawtree, D., Nunes, J. P., Keizer, J. J., Jacinto, R., Santos, J., Rial-Rivas, M. E., & Feger, K. H. (2015). Time series analysis of the long-term hydrologic impacts of afforestation in the Águeda watershed of north-central Portugal. *Hydrology and Earth System Sciences*, 19(7), 3033-3045.

Shao, Q., Li, Z., & Xu, Z. (2010). Trend detection in hydrological time series by segment regression with application to Shiyang River Basin. *Stochastic Environmental Research and Risk Assessment*, 24(2), 221-233.

Kallache, M., Rust, H. W., & Kropp, J. (2005). Trend assessment: applications for hydrology and climate research. *Nonlinear Processes in Geophysics*, 12(2), 201-210.

Yue, S., & Wang, C. (2004). The Mann-Kendall test modified by effective sample size to detect trend in serially correlated hydrological series. *Water resources management*, 18(3), 201-218. Yue, S., Pilon, P., Phinney, B., & Cavadias, G. (2002). The

influence of autocorrelation on the ability to detect trend in hydrological series. *Hydrological processes*, 16(9), 1807-1829.

Yue, S., Pilon, P., Phinney, B., & Cavadias, G. (2002). The influence of autocorrelation on the ability to detect trend in hydrological series. *Hydrological processes*, 16(9), 1807-1829.

Giakoumakis, S. G., & Baloutsos, G. (1997). Investigation of trend in hydrological time series of the Evinos River basin. *Hydrological sciences journal*, 42(1), 81-88.

Salas, J. D. (1980). *Applied modeling of hydrologic time series*. Water Resources Publication.

Hyvärinen, V. (2003). Trends and Characteristics of Hydrological Time Series in Finland: Paper presented at the 13th Northern Res. Basins/Workshop (Saariselkä, Finland and Murmansk, Russia-Aug. 19-24 2001). *Hydrology Research*, 34(1-2), 71-90.